

2

Cone spectral sensitivities and color matching

Andrew Stockman and Lindsay T. Sharpe

The eye's optics form an inverted image of the world on the dense layer of light-sensitive photoreceptors that carpet its rear surface. There, the photoreceptors transduce arriving photons into the temporal and spatial patterns of electrical signals that eventually lead to perception. Four types of photoreceptors initiate vision: The rods, more effective at low light levels, provide our nighttime or scotopic vision, while the three classes of cones, more effective at moderate to high light levels, provide our daytime or photopic vision. The three cone types, each with different spectral sensitivity, are the foundations of our trichromatic color vision. They are referred to as long-, middle-, and short-wavelength-sensitive (L, M, and S), according to the relative spectral positions of their peak sensitivities. The alternative nomenclature red, green, and blue (R, G, and B) has fallen into disfavor because the three cones are most sensitive in the yellow-green, green, and violet parts of the spectrum and because the color sensations of pure red, green, and blue depend on the activity of more than one cone type.

A precise knowledge of the L-, M-, and S-cone spectral sensitivities is essential to the understanding and modeling of normal color vision and "reduced" forms of color vision, in which one or more of the cone types is missing. In this chapter, we consider the derivation of the cone spectral sensitivities from sensitivity measurements and from color matching data.

Univariance. Although the probability that a photon is absorbed by a photoreceptor varies by many

orders of magnitude with wavelength, its effect, once it is absorbed, is independent of wavelength. A photoreceptor is essentially a sophisticated photon counter, the output of which varies according to the number of photons that it absorbs (e.g., Stiles, 1948; Mitchell & Rushton, 1971). Since a change in photon count could result from a change in wavelength, from a change in intensity, or from both, individual photoreceptors are color blind. The visual system is able to distinguish color from intensity changes only by comparing the outputs of two or three cone types with different spectral sensitivities. The chromatic postreceptoral pathways, which difference signals from different cone types (e.g., L-M and $[L + M] - S$), are designed to make such comparisons.

Historical background. The search for knowledge of the three cone spectral sensitivities has a long and distinguished history, which can confidently be traced back to the recognition by Young (1802) that trichromacy is a property of physiology rather than physics (see Chapter 1). But it was only after the revival of Young's trichromatic theory by Helmholtz (1852), and the experimental support provided by Maxwell (1855), that the search for the three "fundamental sensations" or "Grundempfindungen" began in earnest. The first plausible estimates of the three cone spectral sensitivities, obtained by König and Dieterici in 1886 from normal and dichromat color matches, are shown as the gray dotted triangles in Figs. 2.7 and 2.9 later. Their derivation depended on

the “loss,” “reduction,” or “König” hypothesis that protanopes, deuteranopes, and tritanopes lack one of the three cone types but retain two that are identical to their counterparts in normals (Maxwell, 1856, 1860).

Since 1886, several estimates of the normal cone spectral sensitivities have been based on the loss hypothesis, notably those by Bouma (1942), Judd (1945, 1949b), and Wyszecki and Stiles (1967). Here we consider the more recent loss estimates by Vos and Walraven (1971) (which were later slightly modified by Walraven, 1974, and Vos, 1978), Smith and Pokorny (1975) (a recent tabulation of which is given in DeMarco, Pokorny, and Smith, 1992), Estévez (1979), Vos, Estévez, and Walraven (1990), and Stockman, MacLeod, and Johnson (1993) (see Figs. 2.7 and 2.9). Parsons (1924), Boring (1942), and Le Grand (1968) can be consulted for more information on earlier cone spectral sensitivity estimates.

Overview. The study of cone spectral sensitivities now encompasses many fields of inquiry, including psychophysics, biophysics, physiology, electrophysiology, anatomy, physics, and molecular genetics, several of which we consider here. Our primary focus, however, is psychophysics, which still provides the most relevant and accurate spectral sensitivity data.

Despite the confident use of “standard” cone spectral sensitivities, there are several areas of uncertainty, not the least of which is the definition of the mean L-, M-, and S-cone spectral sensitivities themselves. Here we review previous estimates and discuss the derivation of a new estimate based on recent data from monochromats and dichromats. The new estimate, like most previous ones, is defined in terms of trichromatic color matching data.

Several factors, in addition to the variability in photopigments (for which there is now a sound genetic basis; see Chapter 1), can cause substantial individual variability in spectral sensitivity. Before reaching the photoreceptor, light must pass through the ocular media, including the pigmented crystalline lens, and, at the fovea, through the macula lutea, which contains macular pigment. The lens and macular pigments both alter spectral sensitivity by absorbing light mainly of

short wavelengths, and both vary in density between individuals. Another factor that varies between individuals is the axial optical density of the photopigment in the receptor outer segment. Increases in photopigment optical density result in a flattening of cone spectral sensitivity curves. In this chapter, we examine these factors and the effect that each has on spectral sensitivity. Since macular pigment and photopigment optical density decline with eccentricity, both factors must also be taken into account when standard cone spectral sensitivities, which are typically defined for a centrally viewed 2-deg- (or 10-deg-) diameter target, are applied to nonstandard viewing conditions.

Psychophysical methods measure the sensitivity to light entering the eye at the cornea. In contrast, other methods measure the sensitivity (or absorption) of photopigments or photoreceptors with respect to directly impinging light. To compare photopigment or photoreceptor sensitivities with psychophysical ones, we must factor out the effects of the lens and macular pigments and photopigment optical density. We discuss the necessary adjustments and compare the new spectral sensitivity estimates, so adjusted, with data from isolated photoreceptors.

With so much vision research being carried out under conditions of equal luminance, the relationship between the cone spectral sensitivities and the luminosity function, $V(\lambda)$, has become increasingly important. Unlike cone spectral sensitivity functions, however, the luminosity function changes with adaptation. Consequently, any $V(\lambda)$ function of fixed shape is an incomplete description of luminance. We review previous estimates of the luminosity function and present a new one, which we call $V^*(\lambda)$, that is consistent with the new cone spectral sensitivities. Like the previous estimates, however, the new estimate is appropriate only under a limited range of conditions.

What follows is a necessarily selective discussion of cone spectral sensitivity measurements and their relationship to color matching data and luminance, and of the factors that alter spectral sensitivity. Our ultimate goal is to present a consistent set of L-, M-, and S-cone and $V(\lambda)$ spectral sensitivity functions, photopigment optical density spectra, and lens and macular

density spectra that can together be easily applied to predict normal and reduced forms of color vision. We begin with cone spectral sensitivity measurements in normals. (Readers are referred to Chapter 1 for information about the molecular genetics and characteristics of normal and deficient color vision.)

Spectral sensitivity measurements in normals

The three cones types peak in sensitivity in different parts of the spectrum, and their spectral sensitivities overlap extensively (see Figs. 2.2 and 2.12, later). Consequently, spectral sensitivity measurements, in which the threshold for some feature of a target is measured as a function of its wavelength, typically reflect the activity of more than one cone type and often interactions between them. The isolation and measurement of the spectral sensitivity of a single cone type require special procedures to favor the wanted cone type and disfavor the two unwanted ones. Many isolation techniques are based on the two-color threshold technique of Stiles (1939, 1978), so called because the detection threshold for a target or test field of one wavelength is measured on a larger adapting or background field usually of a second wavelength (or mixture of wavelengths). There are two procedures. In the field sensitivity method, a *target* wavelength is chosen to which the cone type to be isolated is relatively sensitive; while in the test sensitivity method, a *background* wavelength is chosen to which it is relatively insensitive.

Field sensitivities. In the field sensitivity method, spectral sensitivity is measured by finding the field radiance that raises the threshold of a fixed-wavelength target by some criterion amount (usually by a factor of ten) as a function of field wavelength. The field sensitivity method was used extensively by Stiles. Through such measurements, and studies of the dependence of target threshold on background radiance for many combinations of target and background wavelength (i.e., threshold versus radiance functions),

he identified seven mechanisms, which he referred to as π -mechanisms.

Although it has been variously suggested that the field sensitivities of some of the π mechanisms, such as π_3 (*S*), π_4 or π'_4 (*M*), and π_5 or π'_5 (*L*), might be the spectral sensitivities of single cones (e.g., Stiles, 1959; Pugh & Sigel, 1978; Estévez, 1979; Dartnall, Bowmaker, & Mollon, 1983), it now seems clear that none reflect the spectral sensitivities of isolated cones. For cone isolation to be achieved using the field sensitivity method requires: (i) that the target is detected by a single cone type at all field wavelengths and (ii) that the threshold for the target is raised *solely* by the effect of the field on that same cone type. The second requirement, of adaptive independence (Boynton, Das, & Gardiner, 1966; Mollon, 1982), fails under many, but not all, conditions (e.g., Pugh, 1976; Sigel & Pugh, 1980; Wandell & Pugh, 1980a, 1980b). Whether adaptive independence holds or not, however, the field spectral sensitivities of Stiles's π -mechanisms, with the exception perhaps of π'_4 , are inconsistent with the cone spectral sensitivities obtained in dichromats and blue-cone (or S-cone) monochromats in some part or parts of the visible spectrum (see below).

Test sensitivities. In the test sensitivity method, the background field wavelength is fixed at a wavelength that selectively suppresses the sensitivities of two of the three cone types but spares the one of interest. Spectral sensitivity is then determined by measuring the target radiance required to detect some feature of the target as a function of its wavelength. Since the background field wavelength and radiance are held constant in a test sensitivity determination, adaptive independence is not a requirement for the test spectral sensitivity to be a cone spectral sensitivity. All that is necessary is target isolation: A single cone type must mediate detection at all test wavelengths.

There have been several attempts to measure complete cone spectral sensitivities using the test sensitivity method, perhaps the most well known of which are those of Wald (1964). Stiles also made extensive test sensitivity measurements but did not publish many of them until 1964, in a paper accompanying Wald's

(Stiles, 1964). A likely reason for his reluctance to publish test spectral sensitivity data was his recognition, which apparently eluded Wald, of the difficulties involved.

In a test sensitivity determination, cone isolation becomes increasingly difficult as the target wavelength approaches the background wavelength. Since the purpose of the background is to maximally suppress the unwanted cone types relative to the cone type to be isolated, its wavelength is typically one to which the wanted cone type is maximally *insensitive* relative to the unwanted cone types. Consequently, when the target wavelength is the same as the background wavelength (as it must be in any complete spectral sensitivity determination), the target works against cone isolation, since it favors detection by the unwanted cones. When the target and background are the same wavelength, the improvement in isolation achieved by the selective suppression of the unwanted cone types by the background is offset by the insensitivity of the wanted cone type to the target. If the sensitivities of the cone types are independently set in accordance with Weber's Law (i.e., if the target threshold rises in proportion to the background intensity), the two factors cancel each other completely: The background raises the thresholds of the unwanted cones, relative to that of the wanted cone, by the *same* amount that the target lowers them. The cone types are then equally sensitive to the target.

Complete isolation can be achieved with the test sensitivity method, but only if the selective sensitivity losses due to adaptation by the background *exceed* the selective effect of the target (King-Smith & Webb, 1974; Stockman & Mollon, 1986). Adaptation, in other words, must exceed Weber's Law independently for each cone type (see Stockman & Mollon, 1986).

(i) *S-cone test sensitivities*: In terms of the spectral range over which cone isolation can be achieved in normal subjects, the test sensitivity method is least successful for S-cone isolation. Even with optimal backgrounds of high intensity, S-cone isolation is possible only from short wavelengths to about 540 nm. S-cone isolation is difficult because S-cone-mediated vision is generally less sensitive than vision mediated

by the M- or L-cones (e.g., Stiles, 1953). The measurement of S-cone test sensitivities throughout the visible spectrum can be achieved with the use of rare blue-cone monochromat observers (see Blue-cone monochromats, below) who lack functioning M- and L-cones. Nevertheless, S-cone spectral sensitivity data measured in color normals obtained over the range over which S-cone isolation is possible remain important as a means of checking the blue-cone monochromat data for abnormalities, which could be introduced, for example, by their typically eccentric fixation.

Figure 2.1 shows S-cone spectral sensitivities (dotted symbols) measured in five normal observers by Stockman, Sharpe, and Fach (1999). The sensitivities are for the detection of a 1-Hz flicker presented on an intense yellow (580-nm) background field that was there to suppress the M- and L-cones and rods. The normal data are consistent with detection by S-cones and with the blue-cone monochromat data (filled symbols) until about 540 nm, after which the M- and L-cones take over target detection. The suggested S-cone spectral sensitivity is indicated in each case by the continuous line.

(ii) *L- and M-cone test sensitivities (steady adaptation)*: A strategy that can be employed to disadvantage detection mediated by S-cones is the use of targets of high temporal and/or spatial frequencies, to which S-cone vision is relatively insensitive (e.g., Stiles, 1949; Brindley, 1954b; Brindley et al., 1966). The use of moderate- to high-frequency heterochromatic flicker photometry (HFP) to measure spectral sensitivity, in which continuously alternating lights of different wavelengths are matched in intensity to minimize the perception of flicker, is also thought to eliminate contributions from the S-cones (Eisner & MacLeod, 1980; but see Stockman, MacLeod, & DePriest, 1991). With S-cone detection disadvantaged, steady chromatic backgrounds can be used to isolate the L-cones from the M-cones, and vice versa, throughout most, but not all, of the visible spectrum. Eisner and MacLeod (1981) found that chromatic backgrounds produced better M-cone or L-cone isolation than predicted by Weber's Law when spectral sensitivity was measured with a 17-Hz HFP. Nevertheless, isolation remains

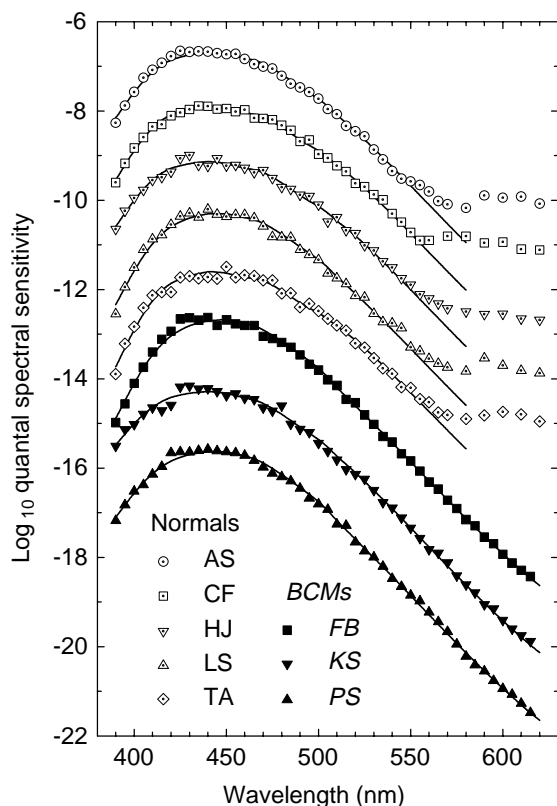


Figure 2.1: Individual 1-Hz spectral sensitivities obtained with central fixation, under S-cone isolation conditions. Each data set, except that for AS, has been displaced vertically for clarity: by -1.2 (CF), -2.0 (HJ), -3.8 (LS), -4.0 (TA), -6.3 (FB), -8.1 (KS), and -9.7 (PS) log units, respectively. Dotted symbols denote observers with normal color vision: AS (circles), CF (squares), HJ (inverted triangles), LS (triangles), and TA (diamonds). Filled symbols denote blue-cone monochromats: FB (squares), KS (inverted triangles), and PS (triangles). The continuous lines drawn through the data are macular- and lens-corrected versions of the Stockman, Sharpe, and Fach (1999) S-cone spectral sensitivities tabulated in the Appendix.

incomplete (Stockman, MacLeod, & Vivien, 1993).

Adaptation with steady fields can exceed Weber's Law by enough to produce M- and L-cone isolation if very small test (3-min-diameter) and background (7-min) fields are used (Stockman & Mollon, 1986). Under such conditions, M- and L-cone adaptation and detection can be monitored separately throughout the

visible spectrum; the resulting M- and L-cone test spectral sensitivities agree well with dichromatic spectral sensitivities and with the cone spectral sensitivities tabulated below (see Appendix, Table 2.1). The main drawback of this technique is the need for very small targets, which makes measurements, especially in naïve subjects, challenging.

(iii) *L- and M-cone test sensitivities (transient adaptation)*: Another way of causing adaptation to exceed Weber's Law is to make the adaptation transient. Stockman, MacLeod, and Vivien (1993) found that temporally alternating the adapting field in both color and intensity suppressed the unwanted cone type sufficiently to isolate either the M- or the L-cone types throughout the visible spectrum. They called this method, in which spectral sensitivity is measured with a 17-Hz flickering target immediately after the exchange of two background fields of different colors, the "exchange" method (see also King-Smith & Webb, 1974). M-cone spectral sensitivity was measured immediately following the exchange from a blue (485-nm) to a deep red (678-nm) field, while L-cone spectral sensitivity was measured following the exchange from a deep red to a blue field. The moderately high flicker frequency and the use of an auxiliary steady, violet background ensured that the S-cones did not contribute to flicker detection.

The mean M-cone spectral sensitivity of 11 normals and 2 protanopes (dotted triangles), and the mean L-cone spectral sensitivity of 12 normals and 4 deuteranopes (dotted inverted triangles) from Stockman, MacLeod, and Johnson (1993) can be compared with the dichromat data of Sharpe et al. (1998) in Figs. 2.2 and 2.10.

Spectral sensitivity measurements in monochromats and dichromats

The isolation and measurement of cone spectral sensitivities is most easily achieved in monochromats and dichromats who lack one or two of the three normal cone types. However, the use of such observers to define normal cone spectral sensitivities requires that

their color vision is truly a “reduced” form of normal color vision (Maxwell, 1860; König & Dieterici, 1886); that is, that their surviving cones have the same spectral sensitivities as their counterparts in color normal trichromat observers.

We can be more secure in this assumption, since it is now possible to sequence and identify the photopigment genes of normal, dichromat, and monochromat observers (Nathans et al., 1986; Nathans, Thomas, & Hogness, 1986) and so distinguish those individuals who conform, genetically, to the “reduction” hypothesis. Yet, factors other than the photopigment type can affect the corneally measured spectral sensitivities (see Factors that influence spectral sensitivity). Thus, it is important, in those spectral regions in which it is possible, to compare the spectral sensitivities of monochromats and dichromats with those of normals. Blue-cone monochromats (Stockman, Sharpe, & Fach, 1999) and protanopes and deuteranopes (Berendschot et al., 1996) may have narrower foveal cone spectral sensitivities than normals, because the photopigment in their foveal cones is lower in density than that in the foveal cones of normals.

Blue-cone monochromats. Blue-cone monochromats (or S-cone monochromats) were first described by Blackwell and Blackwell (1957; 1961), who concluded that they had rods and S-cones but lacked M- and L-cones. Although two psychophysical studies suggested that blue-cone monochromats might also possess a second cone type containing the rod photopigment (Pokorny, Smith, & Swartley, 1970; Alpern et al., 1971), subsequent studies support the original conclusion of Blackwell and Blackwell (Daw & Enoch, 1973; Hess et al., 1989), as does our knowledge of the molecular biology (see Chapter 1).

Spectral sensitivities in blue-cone monochromats of unknown genotype have been measured several times (e.g., Blackwell & Blackwell, 1961; Grützner, 1964; Alpern, Lee, & Spivey, 1965; Alpern et al., 1971; Daw & Enoch, 1973; Smith et al., 1983; Hess et al., 1989), and are typical of the S-cones. Recently, Stockman, Sharpe, and Fach (1999) measured S-cone spectral sensitivities in three blue-cone monochromats

of known genotype. Their results are shown in Fig. 2.1 (filled symbols). The results were obtained in the same way as those for the normal subjects (dotted symbols), except that the flickering target was presented on an orange (620-nm) background of moderate intensity, which was sufficient to saturate their rods.

X-chromosome-linked (red-green) dichromats.

A traditional method of estimating the M- and L-cone spectral sensitivities is to use X-chromosome-linked dichromats, or, as they are also known, red-green dichromats: protanopes, who are missing L-cone function, and deuteranopes, who are missing M-cone function. If the experimental conditions are chosen so that the S-cones do not contribute to sensitivity, L- or M-cone spectral sensitivity can, in principle, be measured directly in such observers.

Protanopes and deuteranopes, however, can each differ in both phenotype and genotype. Some may have one gene in the L- and M-cone photopigment gene array while others may have multiple genes (which yield similar photopigments), and some may have normal photopigment genes while others may have hybrid genes (see Chapter 1).

The estimation of normal L- and M-cone spectral sensitivities from dichromat sensitivities requires the use of protanopes and deuteranopes with normal cone photopigments. There are two slightly different normal L-cone photopigments produced by genes with either alanine [L(ala¹⁸⁰)] or serine [L(ser¹⁸⁰)] at position 180. A similar polymorphism occurs in the M-cone photopigment, but the serine variant is much less frequent than the alanine. The protanope data shown in Figs. 2.2, 2.9, and 2.10 were obtained from subjects who all had alanine at position 180 of their M-cone opsin genes. Strictly speaking, protanopes have hybrid rather than normal M-cone opsin genes, but because the first exons of the L- and M-cone opsin genes are identical, a hybrid L1M2 gene is equivalent to an M-cone opsin gene. A photopigment that is practically indistinguishable from the M-cone photopigment is produced by the hybrid gene L2M3, its λ_{\max} being only 0.2 (Merbs & Nathans, 1992a) or 0.0 nm (Asenjo et al., 1994) different from that of the photopigment

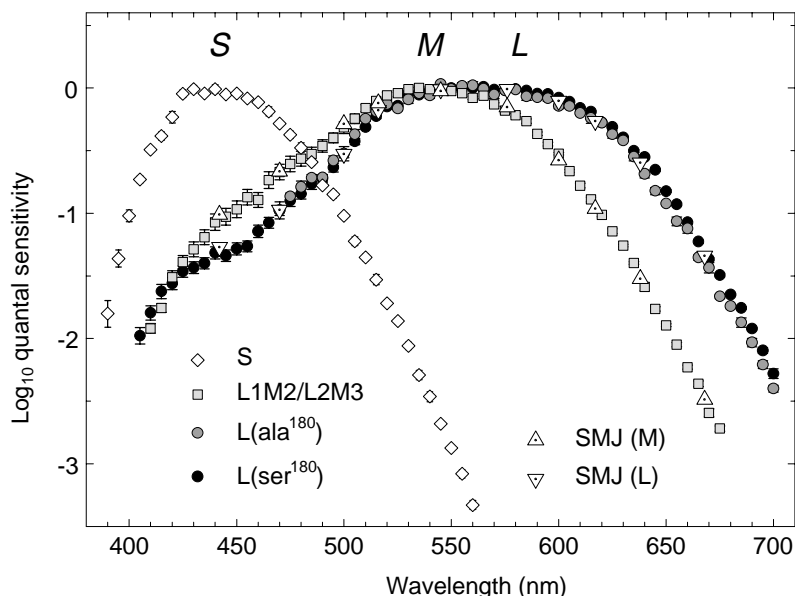


Figure 2.2: Mean spectral sensitivity data. L-cone data from 15 L(ser^{180}) subjects (black circles), 5 L(ala^{180}) subjects (gray circles), and M-cone data from 9 L1M2/L2M3 protanopes (gray squares) measured by Sharpe et al. (1998); and S-cone data from five normals and three blue-cone monochromats (white diamonds) measured by Stockman, Sharpe, and Fach (1999). Also shown are L-cone data from 12 normals and 4 deuteranopes (dotted inverted triangles) and M-cone data for 9 normals and 2 protanopes (dotted triangles) obtained by Stockman, MacLeod, and Johnson (1993).

expressed by the M-cone opsin gene. These values are smaller than the error estimates of the methods used to measure them. Thus, spectral sensitivities from L1M2 and L2M3 protanopes can be reasonably combined.

Dichromats with single photopigment genes in the M- and L-cone pigment gene arrays [L(ala^{180}), L(ser^{180}), L1M2, or L2M3] are especially useful for measuring normal cone spectral sensitivities, because they should possess only a single longer wavelength photopigment. Dichromats with multiple photopigment genes are less useful, unless the multiple genes produce photopigments with the same or nearly the same spectral sensitivities: for example, if an L1M2 or L2M3 gene is paired with an M gene.

With the recent advances in molecular genetics, we can now select protanopes and deuteranopes for spectral sensitivity measurements with the appropriate M- or L-cone photopigment gene(s), as was done in Stockman and Sharpe (2000a) based on the genetic analysis of Sharpe et al. (1998). Some of the protanopes and deuteranopes used in older spectral sensitivity studies (e.g., Pitt, 1935; Hecht, 1949; Hsia & Graham, 1957) may have had hybrid photopigments or multiple longer wavelength photopigments, so that

they are unrepresentative of subjects with normal cone spectral sensitivities.

Figure 2.2 shows the mean data obtained by Sharpe et al. from 15 single-gene deuteranopes with an L(ser^{180}) gene (black circles) and from five single-gene deuteranopes with an L(ala^{180}) gene (gray circles). The spectral sensitivity functions for the two groups are separated by ~ 2.7 nm (Sharpe et al., 1998). Also shown are the data from nine protanopes (gray squares). Of the nine protanopes, three had a single L1M2 gene, three had a single L2M3 gene, one had an L1M2 and an M gene, and two had an L2M3 and an M gene (all genes had alanine at position 180). The mean M- and L-cone data of Stockman, MacLeod, and Johnson (1993) are also shown as the dotted triangles and inverted triangles, respectively. The Stockman, MacLeod, and Johnson data, which are from mainly normals and some dichromats, agree well with the protanope and deuteranope data of Sharpe et al. (1998). Since their group should contain examples of both normal variants of the L-cone photopigment, the mean Stockman, MacLeod, and Johnson L-cone data lie, as expected, between the L(ser^{180}) and L(ala^{180}) means. We will return to the mean spectral sensitivities again

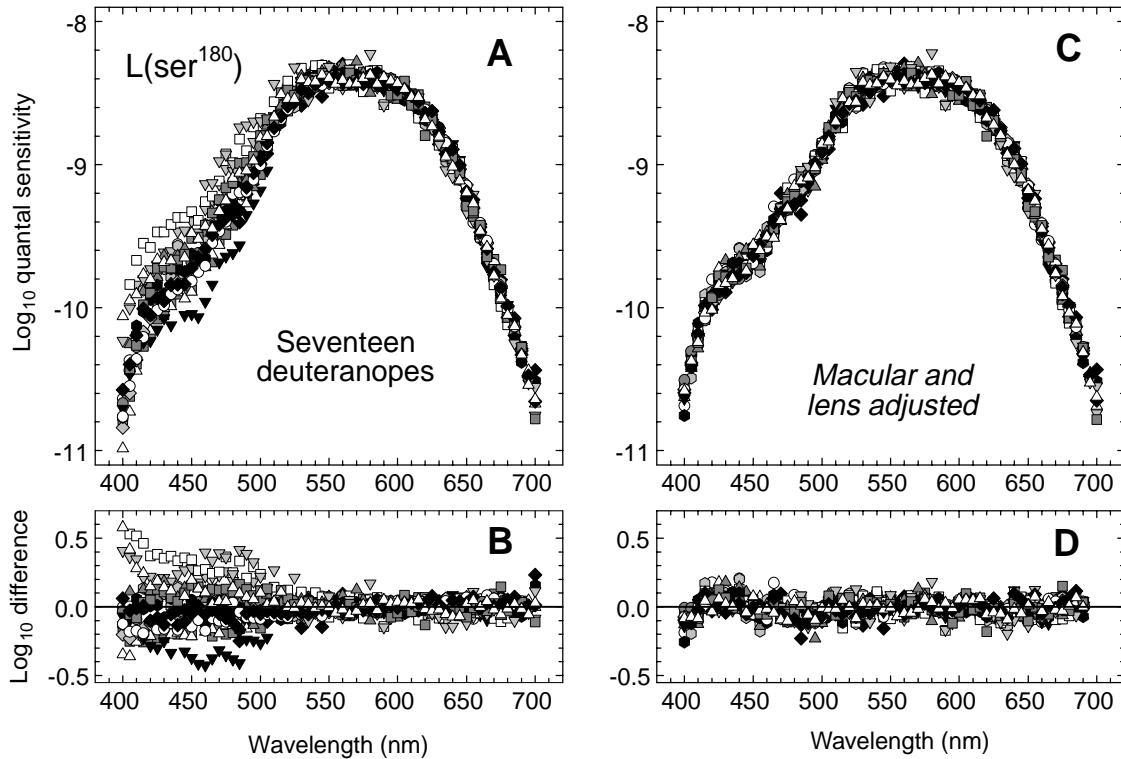


Figure 2.3: Individual differences in macular and lens pigment densities cause individual spectral sensitivity data to appear highly discrepant even if they are determined by the same underlying photopigment. (A) Raw individual L-cone spectral sensitivity data for 17 L(ser¹⁸⁰) observers from Sharpe et al. (1998) vertically aligned with the mean at middle and long wavelengths, and (B) differences between each data set and the mean. (C) Same data individually corrected to best-fitting mean macular and lens optical densities and vertically aligned with mean, and (D) differences between each corrected data set and the mean.

later, when we consider their relationship to color matching data.

Factors that influence spectral sensitivity

Individual spectral sensitivity data can appear highly discrepant, even if they depend on the same underlying photopigment. Examples of the range of differences that are found in actual data are shown in Fig. 2.3, which shows the 17 individual L-cone spectral sensitivities for single-gene deuteranopes with L(ser¹⁸⁰) (Sharpe et al., 1998). Figure 2.3A shows the raw spectral sensitivity data and Fig. 2.3B their differences from the mean.

The main causes of the individual differences seen in Fig. 2.3 are differences in the densities of the macular and lens pigments. We will consider each factor in turn, and also the effect of differences in the density of the photopigment in the cone outer segment. In each case, two issues are important: first, the changes in spectral sensitivity that are caused by variability in each factor; and, second, the effect of each factor on the mean cone spectral sensitivities and color matching data.

Lens density spectra. The lens pigment absorbs light mainly of short wavelengths. The inset of Fig. 2.4A shows three estimates of the lens density spectrum by van Norren and Vos (1974) (open circles); by

Wyszecki and Stiles (1982a) (filled circles); and the slightly modified van Norren and Vos spectrum proposed by Stockman, Sharpe, and Fach (1999) (continuous line). The lens spectrum given in the Appendix to this chapter is that of Stockman, Sharpe, and Fach (1999) for a small pupil. The tabulated densities are correct for the proposed cone fundamentals that are also given in the Appendix. There is evidence that the shape of the lens density spectrum changes with age (e.g., Pokorny, Smith, & Lutze, 1988; Weale, 1988). When unusually young or old groups of subjects or individuals are employed, such changes should be taken into account.

Because of the way in which it was estimated, the “lens pigment” spectrum tabulated in the Appendix, although dominated by the lens pigment itself, is likely to reflect filtering by any other ocular components or perhaps pigments (e.g., Snodderly et al., 1984; Bowmaker et al., 1991) that intervene between the cornea and the photoreceptors and alter spectral sensitivity. The same is true of other lens pigment density spectra, such as the van Norren and Vos (1974) function.

Lens pigment density differences. Individual differences in the density of the lens pigment can be large. One way of estimating lens density differences between observers is to compare their rod spectral sensitivity functions (or scotopic luminosity functions) measured in a macular-pigment free area of the peripheral retina. By assuming that the differences in spectral sensitivity are due to differences in lens density (see Ruddock, 1965), it is possible to estimate the lens density of each observer relative to other observers.

In the 50 observers measured by Crawford (1949) to obtain the mean standard rod spectral sensitivity function, $V(\lambda)$, the range of lens densities was approximately $\pm 25\%$ of the mean density (see van Norren & Vos, 1974). Since lens density increases with the age of the observer (e.g., Crawford, 1949; Said & Weale, 1959), and Crawford’s subjects were under 30, the variability in the general population will be even larger.

Figure 2.4A shows the changes in S-cone spectral sensitivity that result from changes in lens pigment

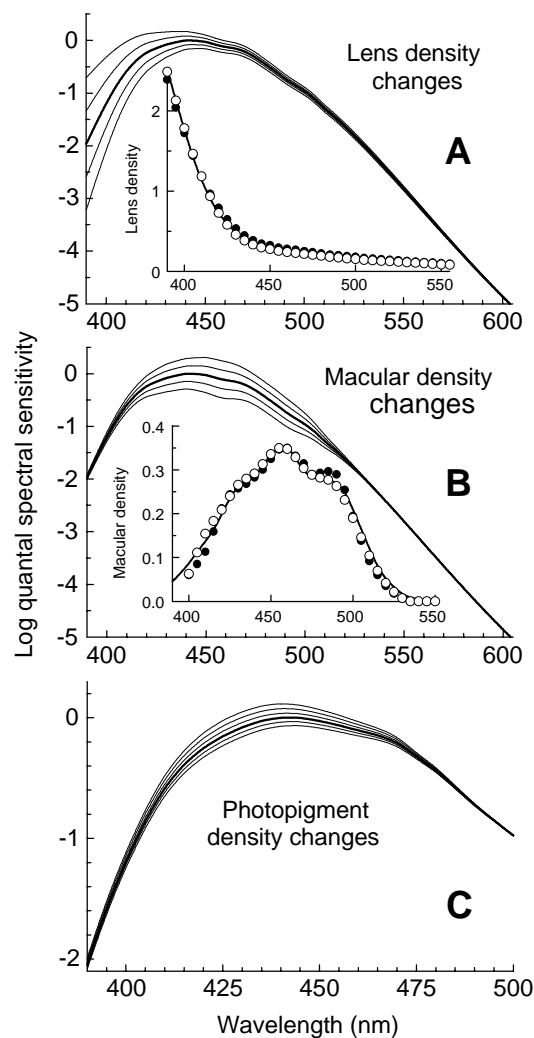


Figure 2.4: Effect on S-cone spectral sensitivity (thick lines) of changes in (A) lens, (B) macular, and (C) photopigment optical densities. (A) From top to bottom, 0.5, 0.75, 1, 1.5, and 2 times the typical lens density. Inset of panel A, lens pigment density spectra of Wyszecki and Stiles (1982a; filled circles), van Norren and Vos (1974; open circles), and the modified version of the van Norren and Vos spectrum proposed by Stockman, Sharpe, and Fach (1999; continuous line, and Appendix). (B) From top to bottom, 0, 0.5, 1, 1.5, and 2 times the typical macular density. Inset of panel B, macular density spectra of Wyszecki and Stiles (1982a; filled circles), Vos (1972; open circles), and one based on Bone, Landrum, and Cains (1992; continuous line, and Appendix). (C) From top to bottom, peak photopigment optical densities of 0.2, 0.3, 0.4 (thick line), 0.5, 0.6, and 0.7. These functions have been normalized at long wavelengths.

density. A typical S-cone spectral sensitivity is indicated by the thickest line, and the effect of varying the lens density in 0.25 steps from one-half the typical density to twice the typical density is indicated by the thinner lines. Changes in lens pigment density variations affect spectral sensitivity mainly at short wavelengths.

Stockman, Sharpe, and Fach (1999) and Sharpe et al. (1998) estimated the lens pigment densities of 40 of their subjects, including those whose data are shown in Figs. 2.1 and 2.3, by measuring rod spectral sensitivities at four wavelengths and comparing the results with the standard rod spectral sensitivity function $V'(\lambda)$. They found that the mean lens densities of their observers was 103.7% of that implied by the $V'(\lambda)$ function with a standard deviation of 16%. The lens density estimates were used to adjust the individual data shown in Fig. 2.3A to the mean lens density value shown in Fig. 2.3C.

Macular density spectrum. The macular pigment also absorbs light mainly of short wavelengths. The inset of Fig. 2.4B shows three estimates of the macular density spectrum by Vos (1972) (open circles); by Wyszecki and Stiles (1982a) (filled circles); and a spectrum (continuous line) based on direct measurements obtained by Bone, Landrum, and Cains (1992). Stockman, Sharpe, and Fach (1999) used the Bone et al. spectrum in their analysis of S-cone spectral sensitivity data, which, in contrast to the Vos (1972) and Wyszecki and Stiles (1982a) spectra, produced plausible estimates of the S-cone photopigment optical density change from central to peripheral retina.

Macular pigment density is typically estimated from the differences between cone spectral sensitivities measured centrally and peripherally, yet both macular pigment density and photopigment optical density vary with eccentricity. Figure 2.5 shows predictions of the L-cone (top panel), M-cone (middle panel), and S-cone (bottom panel) peripheral and central spectral sensitivity differences normalized at long wavelengths. The filled circles show the differences that should be expected if only macular pigment density varies with eccentricity. The lines show the differences

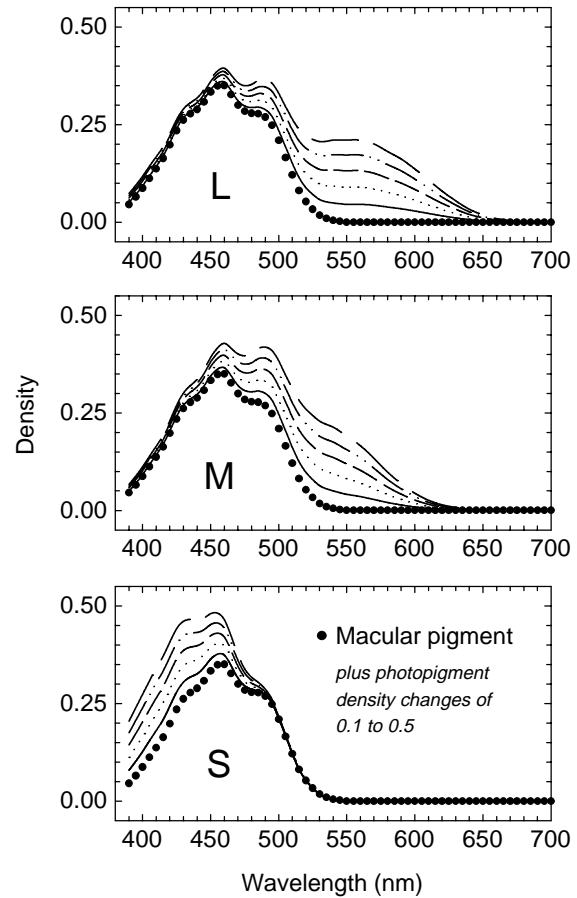


Figure 2.5: Changes in photopigment optical density with eccentricity can substantially distort macular pigment density spectra estimated from peripheral and central spectral sensitivity differences. Predicted differences between peripheral and central spectral sensitivities for a fixed macular pigment spectrum (filled circles, from the Appendix) and peak peripheral and central photopigment optical density differences varying from 0.0 (filled circles) to 0.5 in 0.1 steps for L- (top panel), M- (middle panel), and S- (bottom panel) cone spectral sensitivities (Sharpe et al., 1998).

that should be expected if, *in addition*, the peak photopigment optical density falls by 0.1 from center to periphery (lowest line) to 0.5 from center to periphery (highest line).

The potential dangers of ignoring photopigment density changes with eccentricity can be inferred from Fig. 2.5. For macular pigment density estimates

obtained from peripheral and central sensitivity measurements made at a few wavelengths, photopigment density changes could, depending on the cone type isolated, cause a serious overestimation or underestimation of the actual macular pigment density. For macular estimates obtained from peripheral and central measurements made at several wavelengths, the combined effect of the photopigment and macular density changes could be misinterpreted as a novel macular pigment spectrum (e.g., Pease et al., 1987)

Macular pigment density differences. Individual differences in macular pigment density can also be large: In studies using more than ten subjects, macular pigment density has been found to vary from 0.0 to 1.2 at 460 nm (Wald, 1945; Bone & Sparrock, 1971; Pease, Adams, & Nuccio, 1987). Figure 2.4B shows the changes in S-cone spectral sensitivity that result from changes in macular pigment density, assuming the density spectrum tabulated in the Appendix. A typical S-cone spectral sensitivity is shown by the thick line, and the effect of varying the macular pigment density from zero to twice the typical density (in 0.5 steps) is shown by the thinner lines.

The peak macular density most often assumed at 460 nm is the 0.50 value tabulated in Wyszecki and Stiles (1982a). This value, however, is inappropriate for the standard 2-deg target size that is used to define cone spectral sensitivities. Most macular pigment density determinations, including those on which Wyszecki and Stiles based their estimate, were carried out using fields smaller than 2 deg.

Psychophysically, macular pigment density is most often estimated by comparing spectral sensitivities for a centrally presented target with those for the target presented at an eccentricity of 10 deg or more. Given that macular pigment is wholly or largely absent by an eccentricity of 10 deg (e.g., Bone et al., 1988, Table 2 and p. 847), the change in spectral sensitivity in going from periphery to center can provide an estimate of the macular density spectrum (at the few wavelengths usually measured) and its overall density. This type of estimate is, however, complicated by changes in the

photopigment density between the central and peripheral measurements (see Fig. 2.5).

Nevertheless, several studies have estimated the macular pigment density using 2-deg fields presented centrally and peripherally and have, for simplicity, ignored changes in photopigment optical density. For M- or L-cone-detected lights, Smith and Pokorny (1975) found a mean peak macular density for their 9 subjects (estimated from their Fig. 3) of about 0.36; Stockman, MacLeod, and Johnson (1993) found a mean value of 0.32 for their 11 subjects; and Sharpe et al. (1998) a value of 0.38 for their 38 observers. For S-cone-detected lights, Stockman, Sharpe, and Fach (1999) found a mean value of 0.26 for 5 observers. The mean peak density from these 2-deg studies is approximately 0.35.

Another difficulty that is often ignored is that the macular pigment density over the central 2 deg is likely to be lower for S-cones than for M- and L-cones, since S-cones, unlike M- and L-cones, are absent at the very center of vision, where the macular density is highest, becoming most common at about 1 deg of visual eccentricity (e.g., Stiles, 1949; Wald, 1967; Williams, MacLeod, & Hayhoe, 1981a).

Figure 2.3C shows again the data for the 17 individual L-cone spectral sensitivity curves for single-gene deuteranopes with L(*ser*¹⁸⁰) measured by Sharpe et al. (1998), but now each curve has been adjusted to the mean lens and macular densities using best-fitting estimates of each individual's macular and lens densities. Much of the variability seen in Fig. 2.3A has been removed by the macular and lens density adjustments. The remaining variability is considered below (see Variability in λ_{\max}).

Photopigment optical density. The optical density of the photopigment is related to the axial length of the outer segment in which it resides, the concentration of the photopigment in the outer segment, and the photopigment extinction spectrum (see Knowles & Dartnall, 1977, for further information). Figure 2.4C shows the effects of increasing the peak S-cone photopigment optical density from 0.20 to 0.70 in 0.10 steps. Increases in the photopigment optical density improve

sensitivity least near the photopigment λ_{\max} . As the wavelength decreases or increases away from the λ_{\max} , the sensitivity improvements become larger but reach a constant level at wavelengths far away from the λ_{\max} . To emphasize the changes in the shapes of the spectral sensitivity functions, in Fig. 2.4C we have normalized them at longer wavelengths, where the sensitivity improvement is constant with wavelength.

The photopigment optical density can be estimated from the differences between spectral sensitivities or color matches obtained when the concentration of the photopigment is dilute and those obtained when it is in its normal concentration. This can be achieved psychophysically by comparing data obtained under bleached versus unbleached conditions or for obliquely versus axially presented lights. Estimates can also be obtained by microspectrophotometry (MSP) or from retinal densitometry. Most data refer to the M- and L-cones. Comparing central and peripheral spectral sensitivities is less useful, since macular pigment density, as well as photopigment optical density, declines with eccentricity (see Fig. 2.5). The peak photopigment optical densities referred to here are mainly foveal densities.

(i) *L- and M-cone photopigment optical densities*

(a) Bleaching: In color normals, peak optical density estimates include 0.51 in seven observers (Alpern, 1979); 0.7–0.9 in one observer (Terstiege, 1967); and 0.44 and 0.38, respectively, for the L- and M-cones also in a single observer (Wyszecki & Stiles, 1982b). Two studies have used dichromatic observers. Miller (1972) estimated the peak density to be 0.5–0.6 for the deuteranope and 0.4–0.5 for the protanope, and Smith and Pokorny (1973) found mean peak photopigment densities of 0.4 for four deuteranopes and 0.3 for three protanopes. Burns and Elsner (1993) have obtained mean peak photopigment densities of 0.48 for the L-cones but only 0.27 for the M-cones of six observers.

(b) Oblique presentation: The change in color of monochromatic lights when their incidence on the retina changes from axial to oblique can be accounted for by a self-screening model in which the effective photopigment density is less for oblique incidence (but see Alpern, Kitahara, & Fielder, 1987). Such analyses

have yielded higher estimates of photopigment peak density of between 0.69 and 1.0 (Walraven & Bouman, 1960; Enoch & Stiles, 1961), generally for a 1-deg field.

(c) Direct measures: MSP suggests a specific density in the macaque of $0.015 \pm 0.004 \mu\text{m}^{-1}$ for the M-cones and $0.013 \pm 0.002 \mu\text{m}^{-1}$ for the L-cones (Bowmaker et al., 1978). If we assume a foveal cone outer segment length of 35 μm (Polyak, 1941), these values give axial peak photopigment densities of approximately 0.5 (see Bowmaker & Dartnall, 1980). Retinal densitometry gives a value of 0.35 for the M-cones (Rushton, 1963) and 0.41 for the L-cones (King-Smith, 1973a, 1973b). Recently, Berendschot, van de Kraats, and van Norren (1996), also using retinal densitometry, found mean peak photopigment optical densities of 0.57 in ten normal observers, 0.39 in ten protanopes, and 0.42 in seven deuteranopes.

In summary, with the exception of the work of Terstiege (1967), bleaching measurements yield mean peak optical density values in the range 0.3 to 0.6, Stiles–Crawford analyses in the range 0.7 to 1.0, and objective measures in the range 0.35 to 0.57.

Some evidence now suggests that the optical densities in red-green dichromats may be lower than those in color normals (Berendschot et al., 1996). The resulting separation of data obtained in normals from those obtained in red-green dichromats will lead to a higher estimate of the normal photopigment optical densities. Indeed, for the M- and L-cones, a peak value as high as 0.45 or 0.55 seems appropriate. The mainly color normal M-cone data of Stockman, MacLeod, and Johnson (1993), however, agree well at long wavelengths (see Fig. 2.2) with the protanope data of Sharpe et al. (1998), which suggests that the two groups have similar M-cone photopigment optical densities.

Most of the data reviewed above suggest a lower optical density for M- than for L-cones. Other considerations, however, contradict such a difference. Spectral lights of 548 nm (± 5 nm standard error) retain the same appearance when directly or obliquely incident on the retina, while longer wavelengths appear redder and shorter ones greener (Stiles, 1937; Enoch & Stiles,

1961; Alpern, Kitahara, & Tamaki, 1983; Walraven, 1993). The self-screening model of the change in color with change in the angle of presentation requires that the M- and L-cone photopigment densities are the same at the invariant wavelength. Since the invariant wavelength roughly bisects the M- and L-cone photopigment λ_{\max} wavelengths, their peak photopigment densities must be similar (Stockman, MacLeod, & Johnson, 1993).

(ii) *S-cone photopigment optical density*: All of the evidence reviewed so far has concerned M- and L-cone photopigment optical densities. Not surprisingly, since lights that strongly bleach the S-cone photopigment may be damaging (see Harwerth & Sperling, 1975), there is a lack of information about S-cone photopigment optical density from bleaching experiments.

Stockman, Sharpe, and Fach (1999) estimated the difference in S-cone photopigment optical density and macular pigment density from the changes in S-cone spectral sensitivity between a centrally viewed 2-deg target and the same target viewed at an eccentricity of 13 deg. In addition to changes in macular pigment density, they found differences in peak photopigment optical densities for five normals of 0.19, 0.20, 0.25, 0.26, and 0.26. For three blue-cone monochromats in their study, however, the changes were only -0.04 , -0.01 , and 0.15 ; and the results were consistent with the blue-cone monochromats having central and peripheral photopigment densities that were as low as those found with eccentric presentation in normals. These differences highlight the potential dangers of using spectral sensitivity data from monochromats and dichromats to estimate normal spectral sensitivities. Before being used to define normal spectral sensitivities, the S-cone spectral sensitivity data from blue-cone monochromats were adjusted to normal photopigment and macular pigment densities (Stockman, Sharpe, & Fach, 1999).

Unfortunately, little evidence exists concerning the absolute optical density of the S-cone photopigment, although inferences can be made from anatomical differences between L- and M-cone and S-cone outer segment lengths. In general, the S-cone outer segments are shorter than the L- or M-cone outer segments at the

same retinal location, so that the S-cone optical density should be less than that of the L- or M-cone. Ahnelt (personal communication) suggested that, at the fovea, outer segments of S-cones may be 5% shorter than those of the M- and L-cones; whereas in the periphery, at retinal eccentricities greater than 5 mm (~ 18 deg of visual angle), they may be shorter by 15–20%. In the single electron micrographs showing outer segments, the histological study of Curcio et al. (1991, Fig. 3) indicates that, at a similar parafoveal location, the outer segment of an S-cone (~ 4.1 μm) is almost 40% smaller than that of an L/M-cone (7 μm).

The anatomical data suggest that the S-cone photopigment optical density for the central 2 deg must be less than for the L- or M-cone, but the actual density is uncertain. The 5% difference, suggested by the Ahnelt data, may be too small for our purposes, because the S-cones are absent in the central fovea where the L- and M-cones are longest. A photopigment optical density of somewhere between 5 and 20% lower for the S-cones than for the L- and M-cones could be appropriate for the central 2 deg of vision.

Stockman and Sharpe (2000a) and Stockman, Sharpe, and Fach (1999) assumed mean peak photopigment optical densities of 0.50, 0.50, and 0.40 for the L-, M-, and S-cones, respectively, for the central 2 deg of vision; and 0.38, 0.38 and 0.30, respectively, for the central 10 deg of vision. The absolute densities only minimally affect the cone spectral sensitivity calculations. The relative density changes with eccentricity, however, are critical. They were determined by a comparison of 2-deg and 10-deg CMFs and cone fundamentals (see also Stockman, MacLeod, & Johnson, 1993, Fig. 9C).

Variability in λ_{\max} . Interest in the variability in photopigment λ_{\max} has been revived by the identification of the genes that encode the M- and L-cone photopigments. Estimating the λ_{\max} of the M- and L-cones, like their spectral sensitivities, is easier in red-green dichromats. The most extensive data on the variability in the λ_{\max} of dichromats come from spectral sensitivity measurements done by Matt Alpern and his associates. Alpern and Pugh (1977) reported L-cone

spectral sensitivity curves in eight deuteranopes that varied in λ_{\max} over a total range of 7.4 nm, with a standard deviation of about 2.4 nm. Alpern (1987), analyzing the results from Alpern and Wake (1977) and Bastian (1976), estimated the range of λ_{\max} in 38 protanopes to be 12.4 nm and that in 38 deuteranopes to be 6.4 nm. These ranges are large, yet the standard deviations of the λ_{\max} calculated from Fig. 1 of Alpern (1987) are only 2.3 nm for the protanopes and 1.6 nm for the deuteranopes. Ranges this large would be expected if the red-green dichromats had a mixture of hybrid and normal X-chromosome-linked photopigment genes (see Chapter 1).

From the individual 10-deg color matching data of the 49 color normal observers in the Stiles and Burch (1959) study, MacLeod and Webster (1983), and Webster and MacLeod (1988) estimated the L-cone λ_{\max} values to have a standard deviation of 1.5 nm and the M-cone λ_{\max} values to have a standard deviation of 0.9 nm. MSP data from the eyes of seven persons, however, suggest a greater variability, with standard deviations in λ_{\max} of 3.5 and 5.2 nm, respectively, for 45 human M- and 58 L-cones (Dartnall, Bowmaker, & Mollon, 1983).

Differences in λ_{\max} are to be expected between individuals with different photopigment genes, and it is likely that the observers who made up the λ_{\max} studies so far described differed in photopigment genotype. The difference in photopigment λ_{\max} estimated from the mean L(*ser*¹⁸⁰) and L(*ala*¹⁸⁰) spectral sensitivities shown in Fig. 2.2, for example, is about 2.7 nm (Sharpe et al., 1998). λ_{\max} estimates for other genotypes are noted in Chapter 1.

Also of interest in this context is the variability in the measured λ_{\max} in observers with the *same* photopigment. The data of Sharpe et al. (1998) are useful here, since spectral sensitivities were measured in 17 single-gene L(*ser*¹⁸⁰) deuteranopes. For the 17 observers, the mean estimate of λ_{\max} was 560.14 nm and the standard deviation 1.22 nm (for details, see Sharpe et al., 1998). If these observers had the same photopigment, the variability in λ_{\max} must be due to other factors, such as experimental error, subject error, inappropriate lens and macular corrections, differ-

ences in photopigment optical density, differences in photoreceptor size, differences in photoreceptor orientation, and so on.

Comparable data for the S-cone λ_{\max} comes from the work of Stockman, Sharpe, and Fach (1999). After correcting for lens pigment, macular pigment, and photopigment density differences, they found a mean S-cone photopigment λ_{\max} of 418.8 nm for eight observers and a standard deviation of 1.5 nm. The variability is comparable to that found for the L(*ser*¹⁸⁰) group of observers, and, given that the corrections for the macular and lens pigment differences will add variability to the S-cone λ_{\max} estimates, it is relatively small.

Color matching and cone spectral sensitivities

The trichromacy of individuals with normal color vision is evident in their ability to match any light to a mixture of three independent “primary” lights. The stimuli used in a typical trichromatic color matching experiment are illustrated in the upper panel of Fig. 2.6. The observer is presented with a half-field illuminated by a “test” light of variable wavelength, λ , and a second half-field illuminated by a mixture of the three primary lights. At each λ the observer adjusts the intensities of the three primary lights, which in this example are 645, 526, and 444 nm, so that the test field is perfectly matched by the mixture of primary lights. The results of a matching experiment carried out by Stiles and Burch (1955) are shown in the lower panel of Fig. 2.6, for equal-energy test lights spanning the visible spectrum. The three functions are the relative intensities of the red, green, and violet primary lights required to match the test light λ . They are referred to as the red, green, and “blue” color matching functions (CMFs), respectively, and written $\bar{r}(\lambda)$, $\bar{g}(\lambda)$, and $\bar{b}(\lambda)$.

Although the CMFs shown in Fig. 2.6 are for primaries of 645, 526, and 444 nm, the data can be linearly transformed to any other set of real primary lights and to imaginary primary lights, such as the X,

Y, and Z primaries favored by the CIE or the L-, M-, and S-cone fundamentals or primaries that underlie all trichromatic color matches. Each transformation is accomplished by multiplying the CMFs by a 3×3 matrix. The goal is to determine the unknown 3×3 matrix that will transform the $\bar{r}(\lambda)$, $\bar{g}(\lambda)$, and $\bar{b}(\lambda)$ CMFs to the three cone spectral sensitivities, $\bar{l}(\lambda)$, $\bar{m}(\lambda)$, and $\bar{s}(\lambda)$ (using a similar notation for the cone spectral sensitivities, or “fundamental” color matching functions).

Color matches are matches at the cone level. When matched, the test and mixture fields appear identical to S-cones, to M-cones, and to L-cones. For matched fields, the following relationships apply:

$$(1) \quad \begin{aligned} \bar{l}_R \bar{r}(\lambda) + \bar{l}_G \bar{g}(\lambda) + \bar{l}_B \bar{b}(\lambda) &= \bar{l}(\lambda), \\ \bar{m}_R \bar{r}(\lambda) + \bar{m}_G \bar{g}(\lambda) + \bar{m}_B \bar{b}(\lambda) &= \bar{m}(\lambda), \text{ and} \\ \bar{s}_R \bar{r}(\lambda) + \bar{s}_G \bar{g}(\lambda) + \bar{s}_B \bar{b}(\lambda) &= \bar{s}(\lambda), \end{aligned}$$

where \bar{l}_R , \bar{l}_G , and \bar{l}_B are, respectively, the L-cone sensitivities to the R, G, and B primary lights, and, similarly, \bar{m}_R , \bar{m}_G , and \bar{m}_B are the M-cone sensitivities to the primary lights and \bar{s}_R , \bar{s}_G , and \bar{s}_B are the S-cone sensitivities. We know $\bar{r}(\lambda)$, $\bar{g}(\lambda)$, and $\bar{b}(\lambda)$, and we assume that for a long-wavelength R primary \bar{s}_R is effectively zero, since the S-cones are insensitive in the red. (The intensity of the spectral light λ , which is also known, is equal in energy units throughout the spectrum and so is discounted from the above equations.)

There are therefore eight unknowns required for the linear transformation:

$$(2) \quad \begin{pmatrix} \bar{l}_R & \bar{l}_G & \bar{l}_B \\ \bar{m}_R & \bar{m}_G & \bar{m}_B \\ 0 & \bar{s}_G & \bar{s}_B \end{pmatrix} \begin{pmatrix} \bar{r}(\lambda) \\ \bar{g}(\lambda) \\ \bar{b}(\lambda) \end{pmatrix} = \begin{pmatrix} \bar{l}(\lambda) \\ \bar{m}(\lambda) \\ \bar{s}(\lambda) \end{pmatrix}.$$

Moreover, since we are often unconcerned about the

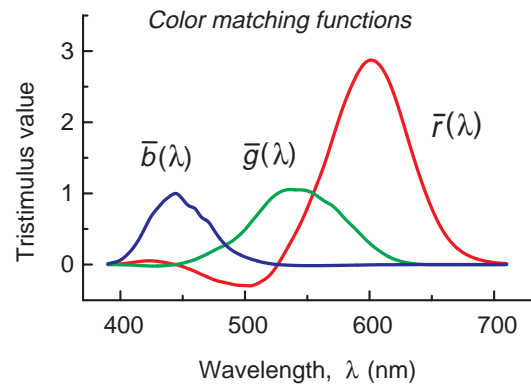
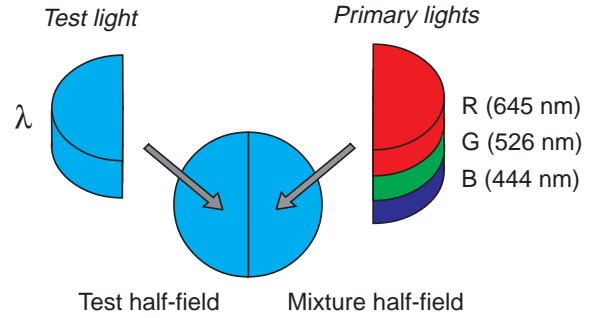


Figure 2.6: A test field of any wavelength (λ) can be matched precisely by a mixture of red (645 nm), green (526 nm), and blue (444 nm) primary lights. The amounts of each of the three primaries or tristimulus values required to match monochromatic lights spanning the visible spectrum are known as the red, $\bar{r}(\lambda)$, green, $\bar{g}(\lambda)$, and blue, $\bar{b}(\lambda)$, color matching functions (red, green, and blue lines, respectively) shown in the lower panel. The data are from Stiles and Burch (1955). A negative sign means that that primary must be added to the target to complete the match. The matching example shown here is actually impossible, since in the blue-green spectral region the red primary is negative. Consequently, it should be added to the target to complete the match, not as shown.

absolute sizes of $\bar{l}(\lambda)$, $\bar{m}(\lambda)$, and $\bar{s}(\lambda)$, the eight unknowns collapse to just five:

$$(3) \quad \begin{pmatrix} \bar{l}_R/\bar{l}_B & \bar{l}_G/\bar{l}_B & 1 \\ \bar{m}_R/\bar{m}_B & \bar{m}_G/\bar{m}_B & 1 \\ 0 & \bar{s}_G/\bar{s}_B & 1 \end{pmatrix} \begin{pmatrix} \bar{r}(\lambda) \\ \bar{g}(\lambda) \\ \bar{b}(\lambda) \end{pmatrix} = \begin{pmatrix} k_l \bar{l}(\lambda) \\ k_m \bar{m}(\lambda) \\ k_s \bar{s}(\lambda) \end{pmatrix},$$

where the absolute values of k_l (or $1/\bar{l}_B$), k_m (or $1/\bar{m}_B$), and k_s (or $1/\bar{s}_B$) remain unknown but are typically chosen to scale three functions in some way: for example, so that $k_l\bar{l}(\lambda)$, $k_m\bar{m}(\lambda)$, and $k_s\bar{s}(\lambda)$ peak at unity. In one formulation (Smith & Pokorny, 1975), $k_l\bar{l}(\lambda) + k_m\bar{m}(\lambda)$ sum to $V(\lambda)$, the luminosity function.

Equations (1) to (3) [and (4) to (6) below] could be for an equal-energy or an equal-quanta spectrum. Since the CMFs are invariably tabulated for test lights of equal energy, we, like previous workers, use an equal-energy spectrum to define the coefficients and calculate the cone spectral sensitivities from the CMFs. We then convert the relative cone spectral sensitivities from energy to quantal sensitivities (by multiplying by λ^{-1}).

The validity of Eqn. (3) depends not only on determining the correct unknowns, but also on the accuracy of the CMFs themselves. There are several CMFs that could be used to derive cone spectral sensitivities. For the central 2-deg of vision, the main candidates are the CIE 1931 functions (CIE, 1932), the Judd (1951) and Vos (1978) corrected version of the CIE 1931 functions, and the Stiles and Burch (1955) functions. Additionally, the 10-deg CMFs of Stiles and Burch (1959), or the 10-deg CIE 1964 CMFs [which are based mainly on the Stiles and Burch (1959) data but also partly on data from Speranskaya (1959), see below] can be corrected to correspond to 2-deg macular and photopigment optical densities.

Color matching data. (i) *CIE 1931 2-deg color matching functions:* The color matching data on which the CIE 1931 2-deg CMFs (CIE, 1932) are based are those of Wright (1928–29) and Guild (1931). Those data, however, are relative color matching data and give only the ratios of the three primaries required to match test lights spanning the visible spectrum. To create color matching functions, however, we also need to know the radiances of the three primaries required for each match. The CIE attempted to reconstruct this information by assuming that a linear combination of the three unknown CMFs must equal the 1924 CIE $V(\lambda)$ function (CIE, 1926) as well as making several other adjustments to the original data (CIE, 1932).

Unfortunately, the validity of the $V(\lambda)$ curve used in the reconstruction is highly questionable. The original sources of short-wavelength luminosity data from which the $V(\lambda)$ curve was derived differed by as much as 10 in the violet (Gibson & Tyndall, 1923; CIE, 1926), and, remarkably, the final derivation at short wavelengths was based on the least sensitive (and least plausible) data (see Fig. 2.13A, later).

Unfortunately, the incorrect CIE 1931 CMFs and the 1924 $V(\lambda)$ function [which is also the $\bar{y}(\lambda)$ CMF of the $\bar{x}(\lambda)$, $\bar{y}(\lambda)$, and $\bar{z}(\lambda)$ transformation of the 1931 CMFs] remain international standards in both colorimetry and photometry.

(ii) *Judd–Vos modified CIE 2-deg color matching functions:* The use of the CIE 1924 $V(\lambda)$ curve to derive the CIE 1931 2-deg CMFs causes a serious underestimation of sensitivity at wavelengths below 460 nm. To overcome this problem, Judd (1951) proposed a revised version of the $V(\lambda)$ function and derived a new set of CMFs [see Wyszecki & Stiles, 1982a, Table 1 (5.5.3)]. Subsequently, Vos made additional corrections to Judd's revision below 410 nm and incorporated the infrared color reversal described by Brindley (1955) to produce the Judd–Vos modified version of the CIE 1931 2-deg CMFs in common usage in color vision research today (Vos, 1978, Table 1). The Judd–Vos modified $V(\lambda)$ function, which is also known as $V_M(\lambda)$, is shown in Fig. 2.13A, later.

The substantial modifications to the CIE 1924 $V(\lambda)$ introduced by Judd are confined mainly to wavelengths below 460 nm, but even above that wavelength [where Judd retained the original CIE 1924 $V(\lambda)$ function] the CIE $V(\lambda)$ function may be incorrect. If the original CIE 1924 luminosity values are too low at and just above 460 nm (as well as at shorter wavelengths, where Judd increased the luminosity values), then the Judd modification creates a “standard” observer whose sensitivity is too low at 460 nm and who could thus be roughly characterized as having artificially high macular pigment density (see Stiles & Burch, 1955, p. 171). Indeed, the Judd modified CIE 2-deg observer does seem to deviate in this way from typical real observers, the Stiles and Burch (1955) 2-deg standard observer, and other relevant data (e.g., Smith,

Pokorny, & Zaidi, 1983; Stockman & Sharpe, 2000a).

The validity of both the Judd–Vos modified CIE 2-deg CMFs and the original CIE 1931 CMFs depends on the assumption that $V(\lambda)$ is a linear combination of the CMFs. This assumption was tested experimentally by Sperling (1958), who measured color matches and luminosity functions in the same observers and found deviations from additivity of up to $0.1 \log_{10}$ unit in the violet, blue, and far-red parts of the spectrum between a flicker-photometric $V(\lambda)$ and the CMFs (see also Stiles & Burch, 1959). This finding suggests that the use of any $V(\lambda)$ function to reconstruct CMFs will result in substantial errors. This problem is compounded in the case of the CIE 1931 functions, because the CIE 1924 $V(\lambda)$ used in their reconstruction was partly determined by side-by-side brightness matches, for which the failures are even greater (Sperling, 1958).

(iii) *Stiles and Burch (1955) 2-deg color matching functions*: Color matching functions for 2-deg vision can be measured directly instead of being reconstructed using $V(\lambda)$. The Stiles and Burch (1955) 2-deg CMFs are an example of directly measured functions. With characteristic caution, Stiles referred to these 2-deg functions as “pilot” data, yet they are the most extensive set of directly measured color matching data for 2-deg vision available, being averaged from matches made by ten observers. A version of the Stiles and Burch (1955) 2-deg CMFs is tabulated in Wyszecki and Stiles (1982a), Table I (5.5.3). There are some indications, however, that the raw color matching data, after correction for a calibration error noted in Stiles and Burch (1959), should be preferred.

Despite the differences between the Stiles and Burch (1955) pilot 2-deg CMFs and the CIE 1931 2-deg CMFs, the CIE chose not to modify or remeasure their 2-deg functions. However, even in relative terms (i.e., as ratios of primaries), and plotted in a way that eliminates the effects of macular and lens pigment density variations, there are real differences between the CIE 1931 and the Stiles and Burch (1955) 2-deg color matching data in the range between 430 and 490 nm. Within that range, the CIE data repeatedly fall *outside* the range of the individual Stiles and Burch data

(see Stiles & Burch, 1955, Fig. 1).

(iv) *Stiles and Burch (1959) 10-deg color matching functions*: The most comprehensive set of color matching data are the “large-field” 10-deg CMFs of Stiles and Burch (1959). Measured in 49 subjects from 392.2 to 714.3 nm (and in 9 subjects from 714.3 to 824.2 nm), these data are probably the most secure set of existing color matching data and are available as individual as well as mean data. For the matches, the luminance of the matching field was kept high to reduce possible rod intrusion, but nevertheless a small correction for rod intrusion was applied (see also Wyszecki & Stiles, 1982a, p. 140). Like the Stiles and Burch (1955) 2-deg functions, the Stiles and Burch (1959) 10-deg functions represent directly measured CMFs and so do not depend on measures of $V(\lambda)$.

(v) *CIE (1964) 10-deg color matching functions*: The large-field CIE 1964 CMFs are based mainly on the 10-deg CMFs of Stiles and Burch (1959) and to a lesser extent on the 10-deg CMFs of Speranskaya (1959). While the CIE 1964 CMFs are similar to the 10-deg CMFs of Stiles and Burch (1959), they differ in ways that compromise their use as the basis for cone fundamentals. First, at short wavelengths, the CIE 1964 functions were artificially extended to 360 nm, which is well beyond the short-wavelength limit of the color matches (392 nm) measured by Stiles and Burch. While a straightforward extrapolation could simply be ignored, the CIE chose to accommodate their extension by making small changes to the CMFs in the measured range. Although less than $0.1 \log_{10}$ unit, the changes conspicuously distort the shape of the cone photopigment spectra derived from CIE 10-deg CMFs at short wavelengths. Second, large adjustments were made to the blue CMF above 520 nm. These changes mean that the CIE 1964 10-deg CMFs cannot be used to derive the S-cone fundamental by finding the ratio of $\bar{b}(\lambda)$ to $\bar{g}(\lambda)$ at middle and long wavelengths (which is possible for the original Stiles and Burch 10-deg functions), and, furthermore, that the CIE 1964 10-deg CMFs cannot be used to define the S-cone fundamental above 520 nm.

(vi) *Conclusions*: Previous estimates of the cone spectral sensitivities are linear transformations of the

Judd modified or Judd–Vos modified CIE 2-deg CMFs (e.g., Vos & Walraven, 1971; Smith & Pokorny, 1975), the Stiles and Burch 2-deg CMFs (e.g., Estévez, 1979; Vos et al., 1990; Stockman, MacLeod, & Johnson, 1993), or the CIE 1964 10-deg CMFs (Stockman, MacLeod, & Johnson, 1993). Those tabulated in Table 2.1 (Appendix) are a linear transformation of the Stiles and Burch (1959) 10-deg CMFs adjusted to a 2-deg viewing field, by correcting for the increases in macular pigment density and photopigment optical density. Either the 2-deg or 10-deg Stiles and Burch CMFs are to be preferred because they were directly measured, and are relatively uncontaminated by adjustments introduced by CIE committees. Such changes, although well intentioned, are often unnecessary and lead to unwanted distortions of the underlying color matching data and the derived cone fundamentals. In the remainder of this chapter, therefore, only the Stiles and Burch 2-deg and 10-deg CMFs are considered.

Previous S-cone fundamentals. Figure 2.7 shows some of the previous estimates of the S-cone fundamental. Those based on the Judd–Vos modified CIE 2-deg CMFs include the identical proposals of Vos and Walraven (1971), as modified by Walraven, 1974, and Vos, 1978 (dashed line) and Smith and Pokorny (1975) (filled circles). Those based on the Stiles and Burch (1955) 2-deg CMFs include Estévez (1979) (dot-dashed line); Vos et al., 1990) (long dashed line); and two, which are not shown, Smith, Pokorny, and Zaidi (1983) and Stockman, MacLeod, and Johnson (1993). An estimate by Stockman, MacLeod, and Johnson (1993), based on the CIE (1964) 10-deg CMFs adjusted to 2 deg and extrapolated beyond 525 nm, is shown as the continuous line. The estimate by König and Dieterici (1886) (dotted inverted triangles) was discussed previously.

The several estimates of the S-cone fundamental can be compared with the recent S-cone threshold data (diamonds) obtained by Stockman, Sharpe, and Fach (1999). Those data suggest that all of the proposed fundamentals shown in Fig. 2.7 are too sensitive at longer wavelengths.

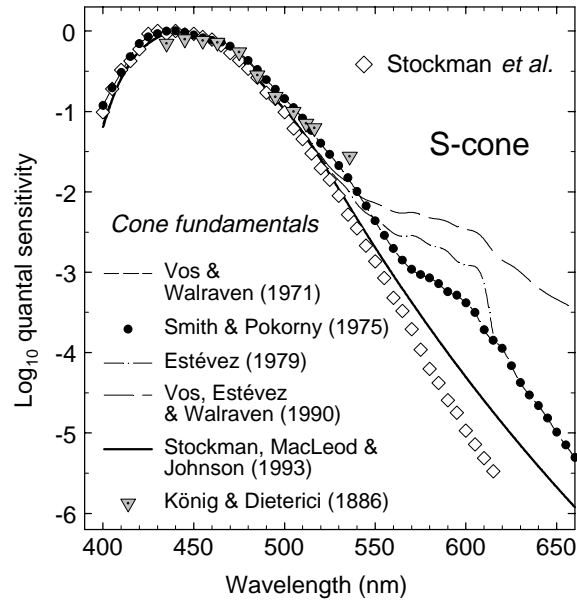


Figure 2.7: Previous estimates of the S-cone spectral sensitivity by König and Dieterici (1886) (dotted inverted triangles); Vos and Walraven (1971) (dashed line); Smith and Pokorny (1975) (filled circles); Estévez (1979) (dot-dashed line); Vos et al. (1990) (long dashed line); and Stockman, MacLeod, and Johnson (1993) (continuous line) compared with the mean S-cone thresholds (open diamonds) of Stockman, Sharpe, and Fach (1999).

New S-cone fundamental. The poor agreement between the threshold data and the proposed S-cone fundamentals shown in Fig. 2.7 led Stockman, Sharpe, and Fach (1999) to derive new S-cone fundamentals in the Stiles and Burch (1955) 2-deg and Stiles and Burch (1959) 10-deg spaces. The derivation of the relative S-cone spectral sensitivity in terms of $\bar{r}(\lambda)$, $\bar{g}(\lambda)$, and $\bar{b}(\lambda)$ involves just one unknown, \bar{s}_G/\bar{s}_B ; thus:

$$(4) \quad \frac{\bar{s}_G}{\bar{s}_B} \bar{g}(\lambda) + \bar{b}(\lambda) = k_s \bar{s}(\lambda).$$

Stockman, Sharpe, and Fach (1999) employed two methods to find \bar{s}_G/\bar{s}_B for the Stiles and Burch (1955) 2-deg CMFs: The first was based on their 2-deg S-cone threshold measurements, and the second was based on the CMFs themselves. The two methods yielded nearly identical results. The second method

was also used to find \bar{s}_G/\bar{s}_B for the Stiles and Burch (1959) 10-deg CMFs.

(i) *Threshold data:* Figure 2.8A shows the mean central S-cone spectral sensitivities (gray circles) measured by Stockman, Sharpe, and Fach (1999). The sensitivities are averaged from normal and blue-cone monochromat data below 540 nm and from blue-cone monochromat data alone from 540 to 615 nm. Superimposed on the threshold data is the linear combination of the Stiles and Burch (1955) 2-deg $\bar{b}(\lambda)$ and $\bar{g}(\lambda)$ CMFs that best fits the data below 565 nm with best-fitting adjustments to the lens and macular pigment densities. The best-fitting function, $\bar{b}(\lambda) + 0.0163\bar{g}(\lambda)$, produces an excellent fit to the data up to 565 nm; thus $\bar{s}_G/\bar{s}_B = 0.0163$.

(ii) *Color matching data:* By using the method explained in Stockman, MacLeod, and Johnson (1993), the unknown value \bar{s}_G/\bar{s}_B can be derived directly from the color matching data (see also Bongard & Smirnov, 1954). This derivation depends on the longer wavelength part of the visible spectrum being tritanopic for lights of the radiances that are typically used in color matching experiments. Thus, target wavelengths longer than about 560 nm, as well as the red primary, are invisible to the S-cones (at higher intensity levels than those used in standard color matching experiments; wavelengths longer than 560 nm would be visible to the S-cones). In contrast, the green and blue primaries are both visible to the S-cones. Targets longer than 560 nm can be matched for the L- and M-cones by a mixture of the red and green primaries, but a small color difference typically remains because the S-cones detect the field containing the green primary. To complete the match for the S-cones, a small amount of blue primary must be added to the field opposite the green primary. The sole purpose of the blue primary is to balance the effect of the green primary on the S-cones. Thus, the ratio of green to blue primary should be negative and fixed at \bar{s}_G/\bar{s}_B , the ratio of the S-cone spectral sensitivity to the two primaries.

Figure 2.8B shows the Stiles and Burch (1955) green, $g(\lambda)$, and blue, $b(\lambda)$, 2-deg chromaticity coordinates (gray squares), which are related to the CMFs by

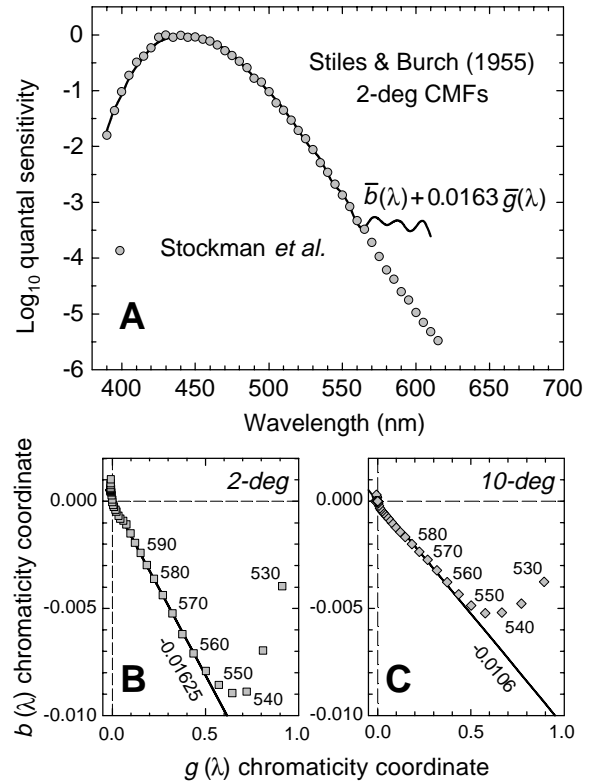


Figure 2.8: (A) Mean central data of Stockman, Sharpe, and Fach (1999) (gray circles) and linear combination of the Stiles and Burch (1955) 2-deg CMFs ($\bar{b}(\lambda) + 0.0163\bar{g}(\lambda)$, continuous line) that best fits them (≤ 565 nm), after applying lens and macular pigment density adjustments. (B) Stiles and Burch (1955) $g(\lambda)$ 2-deg chromaticity coordinates plotted in 5-nm steps against the $b(\lambda)$ chromaticity coordinates (gray squares). The best-fitting straight line from 555 nm to long wavelengths (continuous line) has a slope of -0.01625 . (C) Stiles and Burch (1959) $g(\lambda)$ 10-deg chromaticity coordinates plotted against the $b(\lambda)$ chromaticity coordinates (gray diamonds). The best-fitting straight line from 555 nm to long wavelengths (continuous line) has a slope of -0.0106 .

$g(\lambda) = \bar{g}(\lambda)/[\bar{r}(\lambda) + \bar{g}(\lambda) + \bar{b}(\lambda)]$ and by $b(\lambda) = \bar{b}(\lambda)/[\bar{r}(\lambda) + \bar{g}(\lambda) + \bar{b}(\lambda)]$. As expected, the function above ~ 555 nm is a straight line. It has a slope of -0.01625 , which implies that $\bar{s}_G/\bar{s}_B = 0.01625$. This value is very similar to the value obtained from the direct spectral sensitivity measurements, which supports the adoption of $\bar{b}(\lambda) + 0.0163\bar{g}(\lambda)$ as the S-cone fundamental in the Stiles and Burch (1955) 2-deg

space (Stockman, Sharpe, & Fach, 1999)

Stockman, Sharpe, and Fach (1999) also used the second method to determine the ratio of \bar{s}_G/\bar{s}_B directly for the Stiles and Burch (1959) 10-deg CMFs. Figure 2.8C shows the green, $g(\lambda)$, and blue, $b(\lambda)$, 10-deg chromaticity coordinates (gray diamonds) and the line that best fits the data above 555 nm, which has a slope of -0.0106 . The color matching data suggest that $\bar{b}(\lambda) + 0.0106 \bar{g}(\lambda)$ is the S-cone fundamental in the Stiles and Burch (1959) 10-deg space.

To adjust the 10-deg S-cone fundamental to 2 deg, Stockman, Sharpe, and Fach (1999) assumed a peak photopigment density increase of 0.1 (from 0.3 to 0.4; the absolute densities are not critical in this calculation) and a macular density increase from a peak of 0.095 to one of 0.35. These values were based on analyses of the differences between the original Stiles and Burch 2-deg and 10-deg CMFs; the differences between 2- and 10-deg S-, M-, and L-cone fundamentals derived from the two sets of CMFs and our data; and on calculations from the cone fundamentals back to photopigment spectra.

The 2-deg S-cone fundamental based on the Stiles and Burch (1959) 10-deg CMFs is shown in Fig. 2.12 and is tabulated in the Appendix.

Previous M- and L-cone fundamentals. Figure 2.9 shows previous estimates of the M-cone (A) and L-cone (B) cone fundamentals by Vos and Walraven (1971) (dashed lines); Smith and Pokorny (1975) (filled circles); Estévez (1979) (dot-dashed lines); Vos et al. (1990) (long dashed lines); and Stockman, MacLeod, and Johnson (1993) (continuous lines). For comparison, the mean L1M2/L2M3 (white circles, panel A) and L(ser^{180}) (white squares, panel B) data of Sharpe et al. (1998) are also shown. The estimates by König and Dieterici (1886) (dotted inverted triangles) were described previously.

Both the Vos and Walraven (1971) and the Smith and Pokorny (1975) cone fundamentals are based on the Judd–Vos modified CIE 1931 2-deg CMFs. The crucial difference between them is that in deriving the former it was assumed that $V(\lambda) = \bar{l}(\lambda) + \bar{m}(\lambda) + \bar{s}(\lambda)$, whereas in deriving the latter it was assumed that

$V(\lambda) = \bar{l}(\lambda) + \bar{m}(\lambda)$ (i.e., that the S-cones do not contribute to luminance). Of the two, the Smith and Pokorny (1975) M- and L-cone fundamentals are much closer to the dichromat data at short wavelengths.

The Vos, Estévez, and Walraven (1990) and the Estévez (1979) M- and L-cone fundamentals are based on the Stiles and Burch (1955) 2-deg CMFs. The Estévez (1979) proposal was an attempt to reconcile dichromat spectral sensitivities with Stiles's π_4 and π_5 , but it was a reconciliation for which there was little justification. Vos, Estévez, and Walraven (1990) intended their M-cone fundamental to be consistent with protanopic spectral sensitivities, but clearly it is not. Stockman, MacLeod, and Johnson (1993) also proposed M- and L-cone fundamentals based on the Stiles and Burch (1955) 2-deg CMFs (not shown). Except at short wavelengths, these are similar to the alternative version of the Stockman, MacLeod, and Johnson (1993) M- and L-cone fundamentals that are based on the CIE 1964 10-deg CMFs adjusted to 2 deg, which are shown in Fig. 2.9 (continuous lines).

The comparisons in Fig. 2.9 suggest that the M- and L-cone fundamentals that are most consistent with dichromat data are those of Smith and Pokorny (1975) and Stockman, MacLeod, and Johnson (1993). However, neither estimate agrees perfectly with the new dichromat data provided by Sharpe et al. (1998), even after optimal adjustments in macular and lens pigment densities (Stockman & Sharpe, 1998).

New M- and L-cone fundamentals. The definition of the M- and L-cone spectral sensitivities in terms of $\bar{r}(\lambda)$, $\bar{g}(\lambda)$, and $\bar{b}(\lambda)$ requires knowledge of four unknowns [see Eqn. (3)] \bar{m}_R/\bar{m}_B , \bar{m}_G/\bar{m}_B , \bar{l}_R/\bar{l}_B , and \bar{l}_G/\bar{l}_B ; thus

$$(5) \quad \frac{\bar{m}_R}{\bar{m}_B} \bar{r}(\lambda) + \frac{\bar{m}_G}{\bar{m}_B} \bar{g}(\lambda) + \bar{b}(\lambda) = k_m \bar{m}(\lambda)$$

and

$$(6) \quad \frac{\bar{l}_R}{\bar{l}_B} \bar{r}(\lambda) + \frac{\bar{l}_G}{\bar{l}_B} \bar{g}(\lambda) + \bar{b}(\lambda) = k_l \bar{l}(\lambda).$$

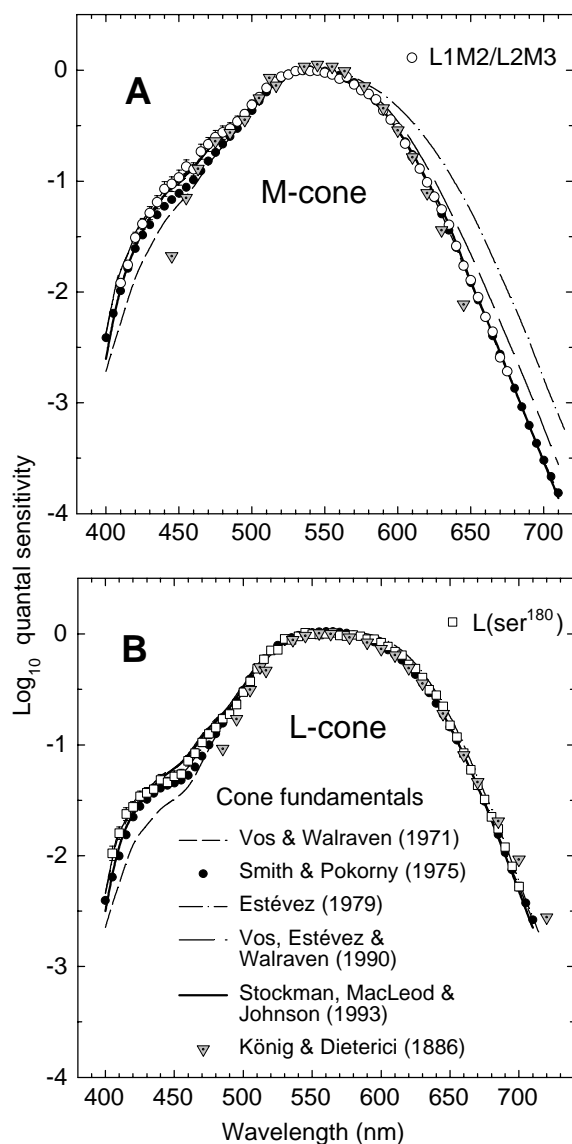


Figure 2.9: Estimates of the M-cone (A) and L-cone (B) fundamentals by König and Dieterici (1886) (dotted inverted triangles); Vos and Walraven (1971) (dashed lines); Smith and Pokorny (1975) (filled circles); Estévez (1979) (dot-dashed lines); Vos et al. (1990) (long dashed lines); and Stockman, MacLeod, and Johnson (1993) (black lines) compared with the mean L1M2/L2M3 (white circles, A) and L(*ser*¹⁸⁰) (white squares, B) data of Sharpe et al. (1998).

Stockman and Sharpe (2000a) used the new red-green dichromat data of Sharpe et al. (1998) to estimate the unknowns in Eqns. (5) and (6), first in terms of the Stiles and Burch (1955) 2-deg CMFs, and then by way of the 2-deg solution in terms of the Stiles and Burch (1959) 10-deg CMFs corrected to 2 deg.

Their strategy, like that of Stockman, MacLeod, and Johnson (1993), was first to find the linear combinations of the Stiles and Burch (1955) 2-deg CMFs that best fit mean spectral sensitivity data. The Stiles and Burch (1955) 2-deg-based cone fundamentals were then used to obtain estimates of the cone spectral sensitivities based on the Stiles and Burch (1959) 10-deg CMFs corrected to 2 deg. In general, color matching data are more precise than threshold data, so it is preferable to define cone spectral sensitivity data in terms of them rather than in terms of the original threshold data.

The linear combinations of the Stiles and Burch (1955) 2-deg CMFs that best fit the mean L(*ser*¹⁸⁰) deuteranope data (open diamonds), L(*ala*¹⁸⁰) deuteranope data (open and filled squares), and L1M2/L2M3 protanope data (open circles) of Sharpe et al. (1998) with macular and lens density adjustments are shown as the continuous lines in Fig. 2.10A. The best-fitting values are given in the figure legend. Figure 2.10B shows the residuals.

The mean Stockman, MacLeod, and Johnson (1993) M-cone data (dotted triangles) and L-cone data (dotted inverted triangles) are also shown in Fig. 2.10A. The M-cone data agree well with the L1M2/L2M3 data, but, at long wavelengths, the L-cone data are slightly steeper than the L(*ser*¹⁸⁰) data and slightly shallower than the L(*ala*¹⁸⁰) data. These differences are expected, because the subjects employed by Stockman, MacLeod, and Johnson have a mixture of L(*ser*¹⁸⁰) and L(*ala*¹⁸⁰) photopigment genes. Consequently, their mean L-cone spectral sensitivity function should be intermediate in spectral position between the mean L(*ser*¹⁸⁰) and L(*ala*¹⁸⁰) functions – as is found.

To derive a normal L-cone spectral sensitivity function from the L(*ser*¹⁸⁰) and L(*ala*¹⁸⁰) data, we needed an estimate of the ratio of L(*ser*¹⁸⁰) to L(*ala*¹⁸⁰) photo-

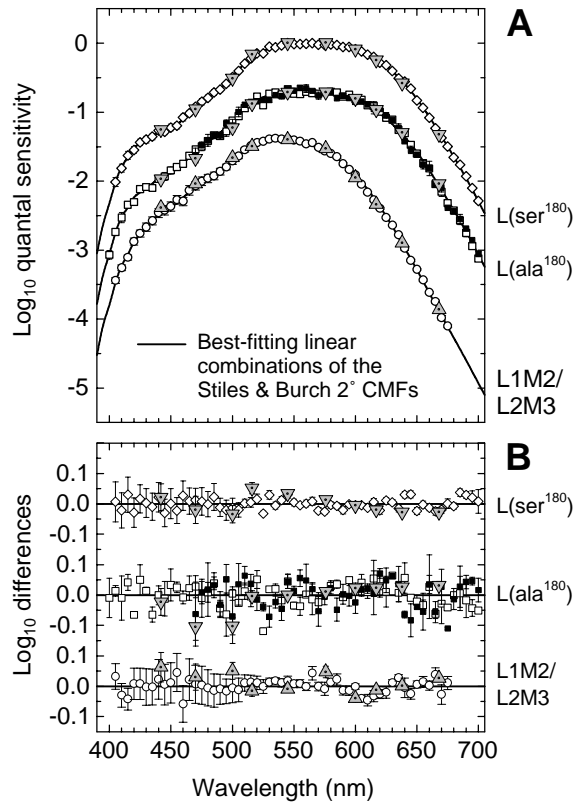


Figure 2.10: Fits of the 2-deg CMFs to dichromat data. (A) Mean L1M2 and L2M3 protanope data (open circles, $n = 9$), and L(ala¹⁸⁰) (open squares, $n = 2$; filled squares $n = 3$) and L(ser¹⁸⁰) (open diamonds, $n = 15$) deutanope data from Sharpe et al. (1998), and the linear combinations of the Stiles and Burch (1955) CMFs (continuous lines) that best fit each set of dichromat data. The dichromat data have been adjusted in macular and lens density to best fit the CMFs. The best-fitting values (ignoring the vertical scaling constant) are $\bar{l}_R/\bar{l}_B = 5.28554$ and $\bar{l}_G/\bar{l}_B = 16.80098$ (L(ser¹⁸⁰), upper line), $\bar{l}_R/\bar{l}_B = 4.15278$ and $\bar{l}_G/\bar{l}_B = 16.75822$ (L(ala¹⁸⁰), middle line), and $\bar{m}_R/\bar{m}_B = 0.29089$ and $\bar{m}_G/\bar{m}_B = 12.24415$ (L1M2/L2M3, lower line). Also shown are the mean M-cone (dotted triangles) and L-cone (dotted inverted triangles) data from Stockman, MacLeod, and Johnson (1993), unadjusted in macular and lens density. (B) Differences between the L1M2/L2M3 data (open circles), L(ala¹⁸⁰) data (open squares), and L(ser¹⁸⁰) data (open diamonds) and the corresponding linear combination of the CMFs, and between the mean M-cone (dotted triangles) or L-cone (dotted inverted triangles) data and the CMFs. Error bars are ± 1 standard error of the mean.

pigments expressed in the normal population. We used the ratio of 0.56 L(ser¹⁸⁰) to 0.44 L(ala¹⁸⁰) found in 308 male Caucasian subjects (see Table 1.2) to determine the mean L-cone fundamental. That is, we set \bar{l}_G/\bar{l}_B and \bar{l}_R/\bar{l}_B to be 0.56 times the L(ser¹⁸⁰) values plus 0.44 times the L(ala¹⁸⁰) ones. Thus, $\bar{l}_G/\bar{l}_B = 16.782165$ and $\bar{l}_R/\bar{l}_B = 4.787127$.

Having derived the L- and M-cone fundamentals in terms of the 2-deg CMFs of Stiles and Burch (1955), we next defined them in terms of the Stiles and Burch (1959) 10-deg CMFs corrected to 2 deg. The 10-deg data set of Stiles and Burch (1959) were used to define the cone fundamentals because they represent the most extensive and secure set of color matching data available. The derivation of the 2-deg M- and L-cone fundamentals as an intermediate step produces relatively smooth and noise-free 2-deg functions that can then be fitted with the adjusted 10-deg CMFs.

We derived the 10-deg-based cone fundamentals by a curve-fitting procedure in which we found the linear combinations of the Stiles and Burch 10-deg CMFs that, after adjustment to 2-deg macular, lens, and photopigment densities, best fit the Stockman and Sharpe 2-deg L- and M-cone fundamentals based on the Stiles and Burch 2-deg CMFs. In making these fits, we assumed a macular pigment density change from a peak of 0.095 for the 10-deg CMFs to a peak of 0.35 for the 2-deg CMFs, a change in lens density from the tabulated values in the Appendix for the 10-deg functions to 92.5% of the tabulated values for the 2-deg functions, and a change in peak photopigment optical density from 0.38 to 0.50 from 10 deg to 2 deg. These are all optimized or best-fitting differences. The best-fitting linear combinations are, for M, $\bar{m}_R/\bar{m}_B = 0.168926$ and $\bar{m}_G/\bar{m}_B = 8.265895$ and, for L, $\bar{l}_R/\bar{l}_B = 2.846201$ and $\bar{l}_G/\bar{l}_B = 11.092490$.

Tritanopic color matches and the M- and L-cone fundamentals. Tritanopic matches provide a useful means of distinguishing between candidate M- and L-cone fundamentals. Since tritanopes lack S-cones, their color matches should be predicted, at least approximately, by any plausible M- and L-cone spectral sensitivity estimates. Stockman, MacLeod, and

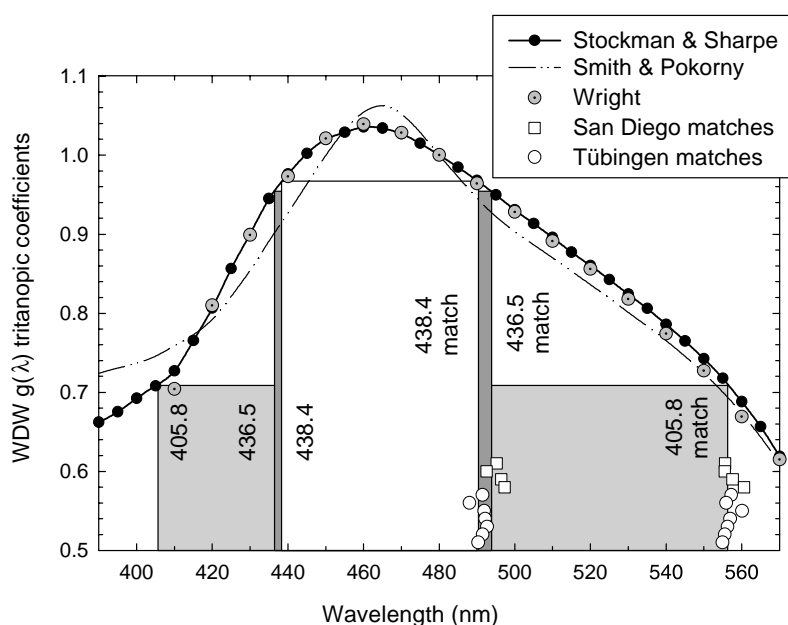


Figure 2.11: Tritanopic color matches and M- and L-cone spectral sensitivities. Tritanopic $g(\lambda)$ predictions of the M- and L-cone fundamentals tabulated in the Appendix (filled diamonds, continuous line); and the wavelengths found by 11 subjects (9 color normals and 2 tritanopes) to match either a 405.8- or a 436.5-nm target light (open squares, San Diego) or a 405.8- or 438.4-nm target light (open circles, Tübingen) under conditions that produce tritanopia in the normals. The matches to the 405.8-, 436.5-, and 438.4-nm lights predicted by the Stockman and Sharpe (2000a) $g(\lambda)$ function are indicated by three large gray or white rectangles. Also shown are Wright's (1952) tritanopic $g(\lambda)$ coefficients (gray dotted circles) and the tritanopic $g(\lambda)$ predictions of the Smith and Pokorny (1975) M- and L-cone fundamentals (dotted-dashed line).

Johnson (1993) actually used the tritanope data of Wright (1952) to substantially adjust their M- and L-cone fundamentals.

Pokorny and Smith (1993) suggested that a simple way to test M- and L-cone fundamentals was to determine the spectral lights that tritanopes confused with the 404.7- and 435.8-nm Hg lines (which, when spectrally isolated, are nearly monochromatic). These two spectral pairs or tritanopic metamers should be predicted by the M- and L-cone spectral sensitivities in question. Following up on their suggestion, Stockman and Sharpe (2000b) carried out matching experiments separately in Tübingen and in San Diego under intense short-wavelength-adapting conditions that produced tritanopia in normals. The matches for five normals and one tritanope measured in Tübingen (open circles) and three normals and one tritanope measured in San Diego (open squares) are shown in Fig. 2.11.

The Hg lines at 404.7 and 435.8 nm are broadened and shifted to longer wavelengths in high-pressure Hg arc lamps (Elenbaas, 1951), so that spectral "lines," after also taking into account the effects of prereceptor filtering, were 405.8 and 438.4 nm in Tübingen (where a filter nominally of 435.8 nm skewed the spec-

tral line to longer wavelengths) and 405.8 and 436.5 nm in San Diego.

The L- and M-cone spectral sensitivities have been plotted in the form of Wright (WDW) $g(\lambda)$ coordinates by transforming them to Wright's primaries of 480 and 650 nm, normalizing them, and setting them to be equal at 582.5 nm [the WDW $r(\lambda)$ coordinates are simply $1 - g(\lambda)$]. Two advantages of plotting the estimates in this way are that WDW coordinates are independent of individual differences in macular and lens pigment densities, and that Wright's (1952) tritanope data (dotted, gray circles) are tabulated in the same form, thus allowing straightforward comparisons. Wright's data, however, are for a target that is more than 50% smaller in area than the 2-deg target and so probably reflect slightly higher L- and M-cone photopigment optical densities.

Figure 2.11 shows the $g(\lambda)$ function (filled diamonds and continuous line) calculated from the L- and M-cone fundamentals (Stockman & Sharpe, 2000a) tabulated in the Table 2.1. The tritanopic matches predicted by the $g(\lambda)$ function are any two wavelengths that have the same $g(\lambda)$ value. As can be seen by following the outlines of the three rectangles from 405.8,

436.5, and 438.4 nm, the Stockman and Sharpe $g(\lambda)$ function predicts the tritanopic matches obtained in Tübingen (open circles) and San Diego (open squares) well, with each predicted match lying within the range of measured matches.

Figure 2.11 also shows the $g(\lambda)$ function predicted by the Smith and Pokorny (1975) fundamentals (dot-dashed line) and Wright's (1952) mean data for seven tritanopes (gray dotted circles). The Smith and Pokorny (1975) predictions agree poorly with Wright's data. The problem lies mainly in the Judd–Vos modified CIE CMFs, which, as others have pointed out, are inconsistent with tritanopic color matching data (Alpern, 1976; Estévez, 1979). The Smith and Pokorny (1975) fundamentals predict the 436.5- and 438.4-nm matches obtained by Stockman and Sharpe (2000b) poorly and the 405.8-nm matches very poorly, missing the mean match by about 12 nm. Stockman, MacLeod, and Johnson (1993) optimized their cone fundamentals to be consistent with Wright's (1952) data. Nevertheless, their predictions (not shown) fail to predict the mean 405.8-nm match found by Stockman and Sharpe (2000b) by about 4.5 nm.

New cone fundamentals

The new S-, M-, and L-cone spectral sensitivities (Stockman & Sharpe, 2000a) are shown in Fig. 2.12 as the continuous lines and are tabulated in the Appendix. They are consistent with spectral sensitivities measured in X-chromosome-linked red-green dichromats, in blue-cone monochromats, and in color normals; they are consistent with tritanopic color matches, and they reflect typical macular pigment and lens densities for a 2-deg field.

The S- (open circles), M- (open inverted triangles), and L- (open squares) cone spectral sensitivities proposed by Smith and Pokorny are also shown in Fig. 2.12. Although they agree with our proposed M- and L-cone spectral sensitivities at middle and long wavelengths, they do not agree at short wavelengths. The agreement between the S-cone functions is poor throughout the spectrum. Large decreases in the mac-

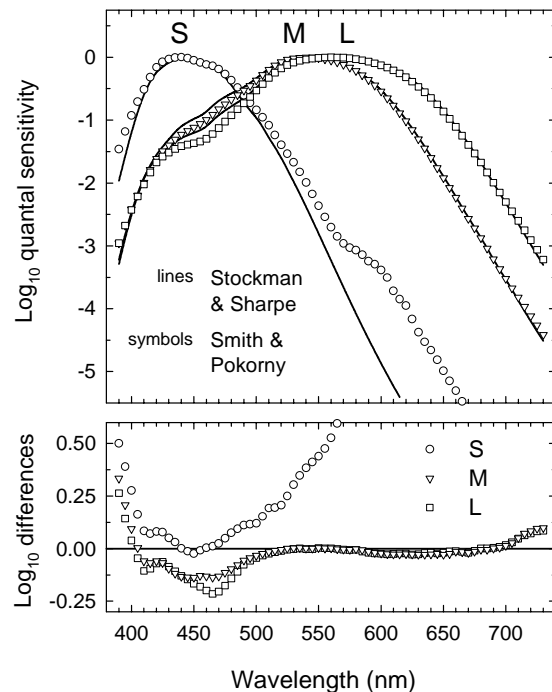


Figure 2.12: (A) S-, M-, and L-cone spectral sensitivity estimates of Stockman and Sharpe (2000a) (continuous lines) compared with the S- (open circles), M- (open inverted triangles), and L- (open squares) cone spectral sensitivity estimates of Smith and Pokorny (1975). (B) Differences between the Smith and Pokorny and Stockman and Sharpe estimates.

ular pigment density of the Smith and Pokorny functions can improve the agreement between the two sets of functions, but the implied macular density of the mean Smith and Pokorny (1975) observer before adjustment is implausibly high for a 2-deg field, and largely artificial.

The luminosity function, $V(\lambda)$

Luminance efficiency is a photometric measure that might loosely be described as “apparent intensity” but is actually defined as the effectiveness of lights of different wavelengths in specific photometric matching tasks. Those tasks now most typically include hetero-

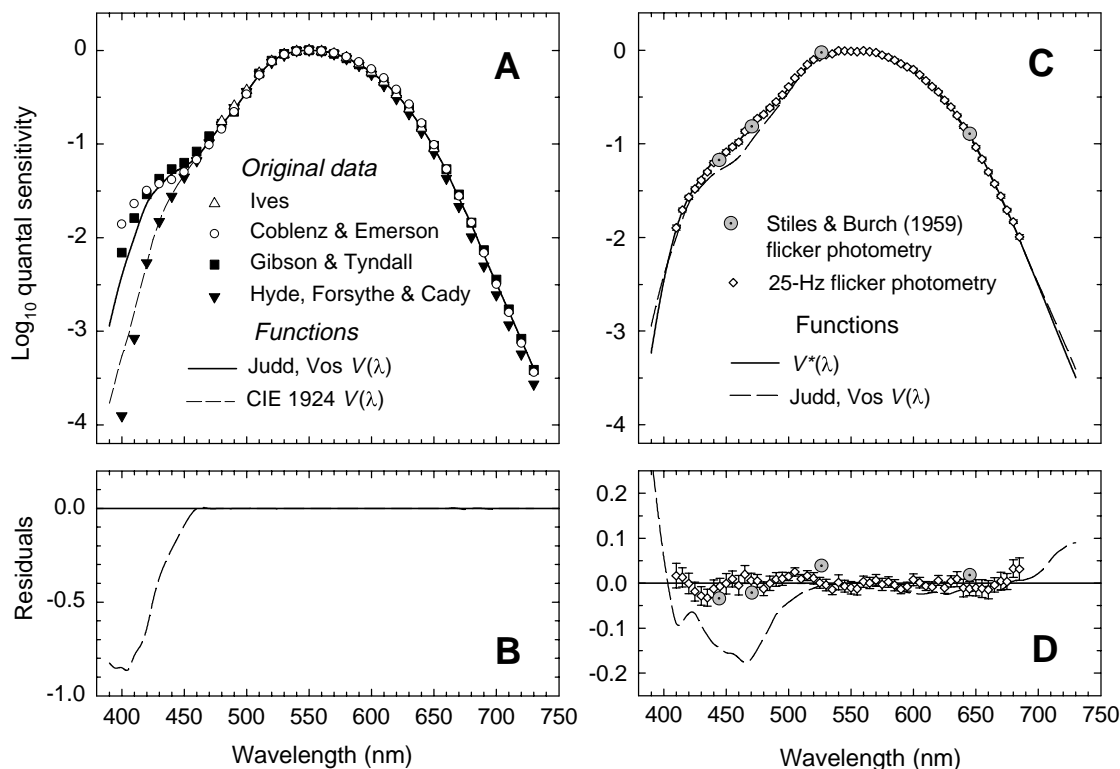


Figure 2.13: (A) The original luminosity measurements by Ives (1912a) (open triangles), Coblenz and Emerson (1918) (open circles), Gibson and Tyndall (1923) (filled squares) and Hyde, Forsythe, and Cady (1918) (filled inverted triangles), which were used to derive the CIE 1924 $V(\lambda)$ function (dashed line), and the Judd–Vos modification to the CIE 1924 $V(\lambda)$ function (continuous line). (B) Differences between the Judd–Vos modified $V(\lambda)$ and the CIE 1924 $V(\lambda)$ functions. (C) $V^*(\lambda)$ (continuous line), the Judd–Vos modified $V(\lambda)$ (dashed line), recent 25-Hz heterochromatic flicker photometric measurements from 22 color normals (open diamonds) used to guide the choice of $V^*(\lambda)$ (Sharpe et al., unpublished observations), and flicker photometric sensitivity measurements by Stiles and Burch (1959) (dotted circles). (D) Differences between the $V^*(\lambda)$ and the other functions shown in (C).

chromatic flicker photometry (HFP), or a version of side-by-side matching, in which the relative intensities of the two half-fields are set so that the border between them appears “minimally distinct” (MDB). Both tasks minimize contributions from the S-cones and produce nearly additive results (e.g., Ives, 1912a; Wagner & Boynton, 1972). So defined, however, luminance is inseparable from the tasks used to measure it.

Previous luminosity functions. The $V(\lambda)$ function, which was adopted by the CIE in 1924 and is still used to define luminance today, was originally pro-

posed by Gibson and Tyndall (1923). It is shown in Fig. 2.13A (short dashed line). The function was based on data obtained by Ives (1912a) (open triangles); Coblenz and Emerson (1918) (open circles); Hyde, Forsythe, and Cady (1918) (filled inverted triangles); and Gibson and Tyndall (1923) (filled squares). Despite the enormous differences between their own data and the proposed standard, Gibson and Tyndall concluded that: “The [older] Illuminating Engineers Society data in the violet have been accepted by the authors for lack of any good reason for changing them, but the relative as well as the absolute values are very

uncertain and must be considered as tentative only.” As a result, the 1924 $V(\lambda)$ function deviates from typical luminosity data (e.g., filled squares, open circles) by a factor of nearly ten in the violet, a problem that continues to plague both colorimetry and photometry 75 years later.

In 1951, Judd proposed a substantial revision to the $V(\lambda)$ function in an attempt to overcome the discrepancies at short wavelengths (Judd, 1951). He retained the older photopic sensitivities at 460 nm and longer wavelengths but increased the sensitivity at shorter wavelengths. Unfortunately, while improving the $V(\lambda)$ function in the violet part of the spectrum, this adjustment artificially created an average observer with implausibly high macular pigment density for a 2-deg field. Vos (1978) subsequently made minor adjustments to the Judd modified CIE $V(\lambda)$ function below 410 nm to produce the Judd–Vos modified CIE $V(\lambda)$ or $V_M(\lambda)$ function (continuous line).

Cone spectral sensitivities and the luminosity function. The luminosity function $V(\lambda)$ falls into a quite different category from cone spectral sensitivities, yet it is often treated as if it were a cone spectral sensitivity. Unlike cone spectral sensitivities, the shape of the luminosity function *changes with adaptation* (e.g., DeVries, 1948b; Eisner & MacLeod, 1981). Thus, any luminosity function is only of limited applicability, because it strictly defines luminance only for the conditions under which it was measured. The function is *not* generalizable to other conditions of adaptation – particularly to other conditions of chromatic adaptation – or necessarily to other measurement tasks. In contrast, cone spectral sensitivities (and CMFs, in general) do not change with adaptation, until photopigment bleaching becomes significant (in which case, the changes reflect the reduction in photopigment optical density). Cone spectral sensitivities are receptorial; the luminosity function is postreceptorial.

Both the L- and M-cones contribute to luminance, although their contribution is typically dominated by the L-cones (e.g., Cicerone & Nerger, 1989; Vimal et al., 1989). The contribution of the S-cones to lumi-

nance has been somewhat contentious, but it now seems clear that the S-cones do make a small contribution (Eisner & MacLeod, 1980; Stockman & MacLeod, 1987; Verdon & Adams, 1987; Lee & Stromeyer, 1989; Stockman, MacLeod, & DePriest, 1991).

Given that the S-cone contribution is so small, and is also so dependent on temporal frequency and adaptation (Stockman, MacLeod, & DePriest, 1991), it is of practical convenience to assume that the S-cone contribution is zero, which is the assumption that we make in deriving $V^*(\lambda)$, the new luminosity function, and it is the assumption that Smith and Pokorny (1975) made in deriving their cone spectral sensitivities. Although convenient, this assumption restricts the validity of any $V(\lambda)$ function to conditions under which S-cone stimulation is small.

Photometry and physiology. The goal in providing a $V(\lambda)$ luminosity function is to construct a spectral sensitivity function that predicts “effective intensity” over the broadest range of conditions. It should be recognized, however, that $V(\lambda)$ is more of a photometric convention than a physiological reality. The $V(\lambda)$ function predicts behavior on HFP and MDB tasks under neutral adaptation and near-threshold. Under these limited conditions, $V(\lambda)$ may even reflect activity in some postreceptorial pathway (e.g., Lee, Martin, & Valberg, 1988). However, under other conditions (for example, with targets of long duration, with large targets, with strongly suprathreshold targets, with short-wavelength targets, and with chromatic adaptation), $V(\lambda)$ is inappropriate. The incorporation of $V(\lambda)$ into color spaces (see below, Two- and three-dimensional color matching and cone spaces) similarly limits the usefulness of those spaces.

To the extent that there is a luminance mechanism, its spectral sensitivity is not, in general, predicted by $V(\lambda)$, since the spectral sensitivity changes with adaptation. To incorporate changes with chromatic adaptation, the spectral sensitivity of the luminance mechanism could be defined as the combination of weighted cone contrasts (see Chapter 18).

$V^*(\lambda)$ luminosity function. Unlike the CIE 2-deg CMFs, the Stiles and Burch (1959) 10-deg CMFs are purely colorimetric and are not connected to any directly measured luminosity function. In some ways this is fortunate, since it prevents the Stiles and Burch based cone spectral sensitivity functions from being altered to be consistent with the prevailing model of $V(\lambda)$, as has happened with the CIE based functions (e.g., Vos & Walraven, 1971; Smith & Pokorny, 1975). In other ways, however, it is unfortunate, since a knowledge of the appropriate luminosity function for the Stiles and Burch based observer is, in many cases, desirable.

Given the differences between the CIE 2-deg and the Stiles and Burch 2- and 10-deg spaces, the CIE $V(\lambda)$ function cannot be used to define luminosity in the Stiles and Burch spaces without introducing large errors into some calculations (such as in the calculation of the MacLeod–Boynton coordinates; see below, Equal-luminance cone excitation space). The known problems of the CIE $V(\lambda)$ functions aside, the CIE functions were, inevitably, measured in different subjects than those used to measure the Stiles and Burch CMFs, so that individual differences play a role.

Instead of $V(\lambda)$, we could use the CIE 1964 estimate of the luminosity function for 10-deg vision [$\bar{y}_{10}(\lambda)$], which we refer to as $V_{10}(\lambda)$, corrected to 2 deg. However, this function is “synthetic,” because it was constructed from luminosity measurements made at only four wavelengths (see Stiles & Burch, 1959). An advantage of the $V_{10}(\lambda)$ function, however, is that it was based on data from some of the same subjects that were used to obtain the Stiles and Burch (1959) 10-deg CMFs.

To define luminance we propose a modified $V(\lambda)$ function, which we refer to as $V^*(\lambda)$, that retains some of the properties of the original CIE $V(\lambda)$ but is consistent with the new cone fundamentals. One property that is retained, which is also a property of the Smith and Pokorny (1975) cone fundamentals and $V(\lambda)$, is that:

$$(7) \quad V^*(\lambda) = a\bar{l}(\lambda) + \bar{m}(\lambda),$$

where a is a scaling constant. The appropriate value of a for the Stockman and Sharpe (2000a) cone fundamentals tabulated in the Appendix could be estimated by finding (i) the linear combination of $\bar{l}(\lambda)$ and $\bar{m}(\lambda)$ that best fits the CIE Judd–Vos $V(\lambda)$ and (ii) the linear combination of $\bar{l}(\lambda)$ and $\bar{m}(\lambda)$ – before their adjustment from 10 to 2 deg – that best fits $V_{10}(\lambda)$, both after macular and lens adjustments. The best-fitting values of a [relative to $\bar{l}(\lambda)$ and $\bar{m}(\lambda)$ having the same peak sensitivities] are 1.65 with a standard error of the fitted parameter of 0.15 for the CIE Judd–Vos $V(\lambda)$ and 1.76 with a standard error of the fitted parameter of 0.05 for $V_{10}(\lambda)$. Alternatively, we can find the linear combination of $\bar{l}(\lambda)$ and $\bar{m}(\lambda)$ that best fits experimentally determined FPS data. Such data, recently obtained in one of our labs for 22 male subjects of known genotype [13 L(S180) and 9 L(A180)] using 25-Hz flicker photometry, are shown in Fig. 2.13C. The mean (open diamonds) has been weighted so that, like the cone spectral sensitivities, it represents a ratio of 0.56 L(ser¹⁸⁰) to 0.44 L(ala¹⁸⁰) (see Table 1.2). After macular and lens adjustments, the best-fitting value of a is 1.50 with a standard error of the fitted parameter of 0.05. (If an S-cone contribution is allowed, the S-cone weight is negative and 0.10% of the L-cone weight.) For consistency with the experimental data, we chose a value of a of 1.50. The definition of $V^*(\lambda)$, therefore, is:

$$(8) \quad V^*(\lambda) = 1.50\bar{l}(\lambda) + \bar{m}(\lambda),$$

again relative to $\bar{l}(\lambda)$ and $\bar{m}(\lambda)$ having the same peak sensitivities. $V^*(\lambda)$ is tabulated in the Appendix and is shown in Fig. 2.13C optimally adjusted in macular and lens densities for agreement with the experimental FPS data. The differences between the macular and lens adjusted $V^*(\lambda)$ and the data are shown in Fig. 2.13D.

Figure 2.13C also shows the 2-deg flicker photometric measurements (dotted circles) made at four wavelengths in 26 of the 49 observers of the Stiles and Burch (1959) 10-deg color matching study, which are also more consistent with $V^*(\lambda)$ than with the CIE Judd–Vos $V(\lambda)$.

Photopigment optical density spectra

Calculating photopigment spectra from corneal spectral sensitivities, and vice versa. The calculation of photopigment optical density spectra from corneal spectral sensitivities is, in principle, straightforward, provided that the appropriate values of (i) D_{peak} – the peak optical density of the photopigment, (ii) k_{lens} – the scaling constant by which the lens density spectrum ($d_{lens}(\lambda)$) should be multiplied, and (iii) k_{mac} – the scaling constant by which the macular density spectrum ($d_{mac}(\lambda)$) should be multiplied are known. Starting with the *quantal* spectral sensitivity of, for example, the L-cones ($\bar{l}(\lambda)$), the effects of the lens pigment ($k_{lens}d_{lens}(\lambda)$) and the macular pigment ($k_{mac}d_{mac}(\lambda)$) are first removed, by restoring the sensitivity losses that they cause:

$$(9) \quad \log(\bar{l}_p(\lambda)) = \log(\bar{l}(\lambda)) + k_{lens}d_{lens}(\lambda) + k_{mac}d_{mac}(\lambda).$$

The functions $d_{lens}(\lambda)$ and $d_{mac}(\lambda)$ are the optical density spectra of the lens and macular tabulated in the Appendix. They are scaled to the densities that are appropriate for the Stockman and Sharpe (2000a) 2-deg cone fundamentals that are also tabulated there (0.35 macular density at 460 nm and 1.765 lens density at 400 nm). Thus, the values k_{lens} and k_{mac} are 1.0 for the mean fundamentals, but should be adjusted for individual observers or groups of observers with different lens and macular densities. $\bar{l}_p(\lambda)$ is the spectral sensitivity of the L-cones at the photoreceptor level.

To calculate the photopigment optical density of the L-cones scaled to unity peak ($\bar{l}_{OD}(\lambda)$), from $\bar{l}_p(\lambda)$:

$$(10) \quad \bar{l}_{OD}(\lambda) = \frac{-\log(1 - \bar{l}_p(\lambda))}{D_{peak}}.$$

We assumed D_{peak} , the peak optical density, to be 0.5, 0.5, and 0.4 for the L-, M-, and S-cones, respectively [$\bar{l}_p(\lambda)$ should be scaled before applying Eqn. (10), so that $\bar{l}_{OD}(\lambda)$ peaks at unity]. These calculations from corneal spectral sensitivities to retinal photopigment optical densities ignore changes in spectral sensitivity that may result from the structure of the

photoreceptor or other ocular structures and pigments (unless they are incorporated in the lens or macular pigment density spectra).

The calculation of relative quantal corneal spectral sensitivities from photopigment or absorbance spectra is also straightforward, again if the appropriate values (D_{peak} , k_{lens} , and k_{mac}) are known. First, the spectral sensitivity at the photoreceptor level, $\bar{l}_p(\lambda)$, is calculated from the normalized photopigment optical density spectrum, $\bar{l}_{OD}(\lambda)$, by the inversion of Eqn. (10) (see Knowles & Dartnall, 1977):

$$(11) \quad \bar{l}_p(\lambda) = 1 - 10^{-D_{peak}\bar{l}_{OD}(\lambda)}.$$

Then, the filtering effects of the lens and macular pigments are added back:

$$(12) \quad \log(\bar{l}(\lambda)) = \log(\bar{l}_p(\lambda)) - k_{lens}d_{lens}(\lambda) - k_{mac}d_{mac}(\lambda).$$

The lines in Fig. 2.14 are the logarithm of the photopigment optical densities, $\bar{l}_{OD}(\lambda)$, $\bar{m}_{OD}(\lambda)$, and $\bar{s}_{OD}(\lambda)$, calculated using Eqns. (9) and (10) from the cone fundamentals tabulated in the Appendix (Table 2.1). The photopigment optical densities are also tabulated in the Appendix.

Scales. Attempts have been made to simplify cone photopigment spectra by finding an abscissa that produces spectra of a fixed spectral shape, whatever the photopigment λ_{max} . An early proposal was by Dartnall (1953), who proposed a “nomogram” or fixed template shape for photopigment spectra plotted as a function of wavenumber ($1/\lambda$, in units of cm^{-1}). Another proposal was that the spectra are shape-invariant when plotted as a function of \log_{10} frequency or wavenumber [$\log_{10}(1/\lambda)$] (Mansfield, 1985; MacNichol, 1986), which is equivalent to \log_{10} wavelength [$\log_{10}(\lambda)$] or normalized frequency (λ_{max}/λ). For this scale, Lamb (1995) has proposed a template (see Chapter 3). Barlow (1982) has also proposed an abscissa of the fourth root of wavelength ($\sqrt[4]{\lambda}$). The three photopigment spectra (Appendix, Table 2.1) are most similar in shape when plotted against log wavelength.

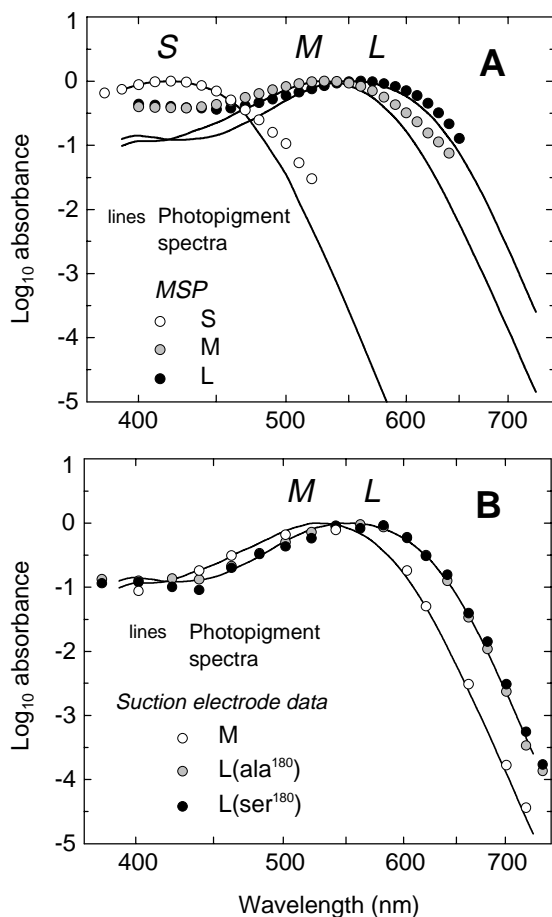


Figure 2.14: Psychophysical estimates of the photopigment optical density spectra compared with direct measurements. Log₁₀ S-, M-, and L-cone photopigment spectra calculated from the Stockman and Sharpe cone fundamentals (continuous lines, Appendix) and (A) human S- (white circles), M- (gray circles), and L-cone (black circles) MSP measurements by Dartnall, Bowmaker, and Mollon (1983) or (B) human M-cone (white circles) suction electrode measurements by Kraft (personal communication), and L(ala¹⁸⁰) cone (gray circles) and L(ser¹⁸⁰) cone (black circles) suction electrode measurements by Kraft, Neitz, and Neitz (1998).

Direct methods of determining photopigment spectra. There are several direct methods of measuring photopigment spectra, only two of which we will consider in any detail. A promising new approach is to produce the cone pigment apoprotein in tissue culture

cells transfected with the corresponding complementary DNA clones and then, after reconstitution of the apoprotein with 11-*cis* retinal, to measure the bleaching difference spectrum in solution (Merbs & Nathans, 1992a; Asenjo, Rim, & Oprian, 1994). As yet, the technique is too noisy to be useful in predicting corneal spectral sensitivities. Moreover, the technique adds another level of uncertainty into the reconstruction of corneal spectral sensitivities from photopigment spectra, since, unlike the other techniques described in this section, the photopigment is not embedded in the photoreceptor membrane. The incorporation of the photopigment into the membrane may change its spectral sensitivity.

Two methods have yielded human photopigment spectra that have frequently been compared with corneally measured spectral sensitivity functions: microspectrophotometry and suction electrode recordings.

(i) *Microspectrophotometry*: In MSP work, the spectral transmission of a small measuring beam passed transversely through the outer segment of a single cone is compared with that of a reference beam passed outside the cone to derive the absorption spectrum of the outer segment (e.g., Bowmaker et al., 1978). Of interest here are the MSP measurements of Dartnall, Bowmaker, and Mollon (1983) of photoreceptors “from the eyes of seven persons.” Figure 2.14A, which compares the MSP results (circles) with the photopigment optical density spectra from the Appendix, Table 2.1 (lines), makes it clear that MSP is of little use in estimating cone spectral sensitivities far away from the photopigment λ_{\max} , because the MSP functions are much too broad. Nonetheless, the comparisons support the use of MSP for defining photopigment λ_{\max} .

(ii) *Suction electrode recordings*: In suction electrode recordings, a single human or primate cone outer segment is drawn inside a small glass electrode and its current response to light is recorded (e.g., Baylor, Nunn, & Schnapf, 1984; 1987). Spectral sensitivity is obtained by finding, as a function of wavelength, the radiance required to elicit a criterion photocurrent response (see Chapter 4).

Relevant human suction electrode data have so far been obtained only from M- and L-cones (Schnapf, Kraft, & Baylor, 1987; Kraft, Neitz, & Neitz, 1998). Recently, Kraft, Neitz, and Neitz (1998) made measurements in human L-cones known to contain photopigments that are determined either by L(*ser*¹⁸⁰) or by L(*ala*¹⁸⁰) genes, and Kraft (personal communication) has made measurements in human M-cones. Their M (white circles), L(*ala*¹⁸⁰) (gray circles), and L(*ser*¹⁸⁰) (black circles) data are shown in Fig. 2.14B along with the photopigment spectra from the Appendix (lines).

Given the differences between the two methods of obtaining the photopigment spectra and the fact that no attempt has been made to improve the agreement between the data sets, the agreement, particularly at shorter wavelengths, is good. At longer wavelengths, the L(*ala*¹⁸⁰) suction electrode data agree well with the corneally derived L-cone photopigment spectrum, but the M and L(*ser*¹⁸⁰) suction electrode data are slightly shallower than the corneally derived M- and L-cone spectra. Such differences have been encountered before, but they have been minimized by assuming unusually low photopigment densities for the central 2 deg of vision (Baylor, Nunn, & Schnapf, 1987) or by comparing them with corneally measured spectral sensitivities that are unusually shallow at longer wavelengths (Nunn, Schnapf, & Baylor, 1984; Baylor, Nunn, & Schnapf, 1987). The differences at long wavelengths may be due to waveguiding.

Waveguides. In both microspectrophotometry and suction electrode recordings the spectral sensitivity of the photopigment is measured transversely through the isolated cone outer segment, rather than axially along the outer segment, as in normal vision. The disadvantage of both methods is that the results must be adjusted before they can be used to predict corneal spectral sensitivities. Factors such as macular, lens, and photopigment density can be corrected for with some certainty, but other less well-known factors, such as other filters (e.g., Snodderly et al., 1984) or waveguide effects, cannot.

Light is transmitted along the photoreceptor in patterns called waveguide modal patterns (see Fig. 6 of

Enoch, 1963). The fraction of the power of each modal pattern that is transmitted inside the photoreceptor to its power outside the photoreceptor decreases with the wavelength of the incident light, so that, in principle, the structure of the photoreceptor can change its spectral sensitivity (see, for example, Enoch, 1961; Enoch & Stiles, 1961; Snyder, 1975; Horowitz, 1981). It is difficult to know precisely how waveguide factors influence the spectral sensitivity for axially incident light in the human fovea because many of the relevant quantities, such as the refractive indices inside and outside the cone outer segment, and the models themselves are uncertain. Assuming values of 1 μm for the diameter of a human foveal cone outer segment (Polyak, 1941) and 1.39 and 1.35, respectively, for the refractive indices inside and outside the cone outer segment (Fig. 6.11 of Horowitz, 1981), standard formulas [Eqn. (7a) and Fig. 9 of Snyder, 1975] suggest a loss of spectral sensitivity for mode η_{11} (the most important mode for axially incident light) of about 0.2 \log_{10} unit for red light relative to violet. Waveguide effects of this magnitude could account for the differences between the suction electrode data and the corneally measured photopigment spectra shown in Fig. 2.14B.

Two- and three-dimensional color matching and cone spaces

The representation of color matching functions and/or cone fundamentals in various two-dimensional (2D) or three-dimensional (3D) spaces can be a vital aid to interpreting and calculating color mixtures, complementary wavelengths, dichromatic confusion colors, chromatic adaptation and discrimination data, and even the behavior of postreceptoral mechanisms (see Chapters 1 and 18).

Color matching data or cone spectral sensitivities are often simplified by plotting them in relative units called chromaticity coordinates. Chromaticity coordinates ($r(\lambda)$, $g(\lambda)$, and $b(\lambda)$) are related to the CMFs ($\bar{r}(\lambda)$, $\bar{g}(\lambda)$, and $\bar{b}(\lambda)$) as follows:

$$(13) \quad r(\lambda) = \frac{\bar{r}(\lambda)}{\bar{r}(\lambda) + \bar{g}(\lambda) + \bar{b}(\lambda)},$$

$$g(\lambda) = \frac{\bar{g}(\lambda)}{\bar{r}(\lambda) + \bar{g}(\lambda) + \bar{b}(\lambda)}, \text{ and}$$

$$b(\lambda) = \frac{\bar{b}(\lambda)}{\bar{r}(\lambda) + \bar{g}(\lambda) + \bar{b}(\lambda)}.$$

Given that $r(\lambda) + g(\lambda) + b(\lambda) = 1$, only $r(\lambda)$ and $g(\lambda)$ are typically plotted, since $b(\lambda)$ is $1 - (r(\lambda) + g(\lambda))$. [Likewise, $l(\lambda)$, $m(\lambda)$, and $s(\lambda)$ are the cone chromaticity coordinates corresponding to the cone fundamentals $\bar{l}(\lambda)$, $\bar{m}(\lambda)$ and $\bar{s}(\lambda)$.]

RGB (or XYZ) color spaces. Figure 2.15A shows the chromaticity coordinates (continuous line) of the locus of monochromatic spectral lights (or “spectrum locus”) in the Stiles and Burch (1955) 2-deg $r(\lambda)$, $g(\lambda)$ chromaticity space. Selected wavelengths are shown as open circles. The Stiles and Burch (1955) based 2-deg cone fundamentals of Stockman and Sharpe (2000a), the derivation of which was discussed above, are plotted in terms of $r(\lambda)$ and $g(\lambda)$ as the dotted diamond (L), circle (M), and square (S).

Although chromaticity coordinates are a convenient way of plotting spectral distributions and predicting color mixtures, they inevitably reduce the available information by projecting the three-dimensional color space onto the two-dimensional plane: $\bar{r}(\lambda) + \bar{g}(\lambda) + \bar{b}(\lambda) = 1$. Figure 2.15B shows the Stiles and Burch (1955) $\bar{r}(\lambda)$, $\bar{g}(\lambda)$, and $\bar{b}(\lambda)$ color matching space and the L- (solid line), M- (long dashed line), and S- (short dashed line) cone vectors. The equal-energy spectrum locus is shown by the solid line, and selected wavelengths are shown by the filled circles. In three dimensions, the relationship between the cone fundamentals and the spectrum locus can be seen more clearly.

LMS color space. Color spaces are much more straightforward and intuitive when they are defined by

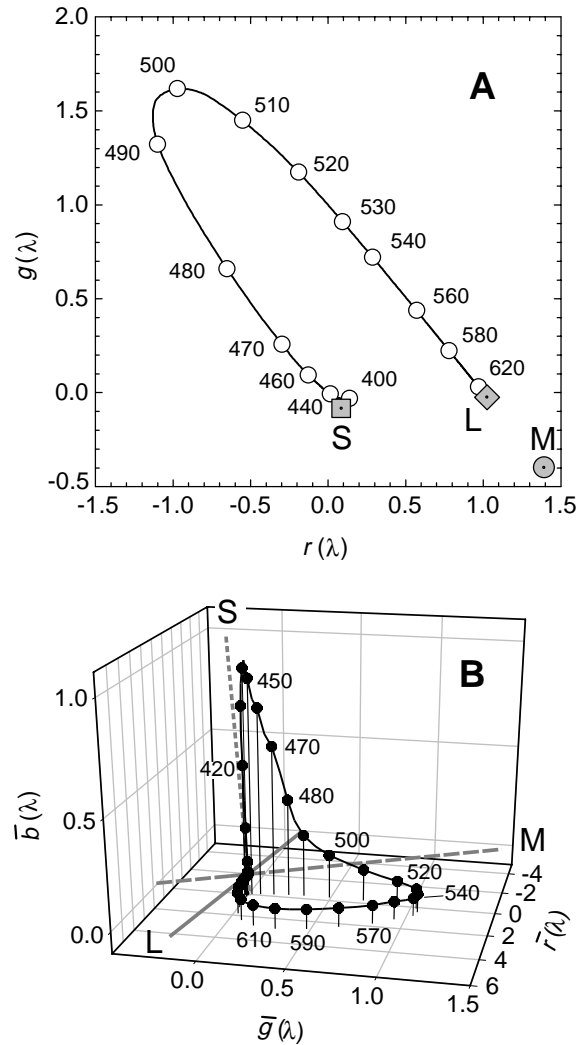


Figure 2.15: Color matching functions and chromaticity coordinates. (A) Spectrum locus (continuous line) and selected wavelengths (open circles) plotted in the Stiles and Burch (1955) 2-deg $r(\lambda)$, $g(\lambda)$ chromaticity space, and the projection of the 2-deg L- (dotted diamond), M- (dotted circle), and S- (dotted square) cone fundamentals of Stockman and Sharpe (2000a). (B) Spectrum locus (continuous line) and selected wavelengths (filled circles) plotted in the Stiles and Burch (1955) 2-deg $\bar{r}(\lambda)$, $\bar{g}(\lambda)$ and $\bar{s}(\lambda)$ space, and the L- (solid gray line), M- (long-dashed gray line), and S- (short-dashed gray line) cone vectors.

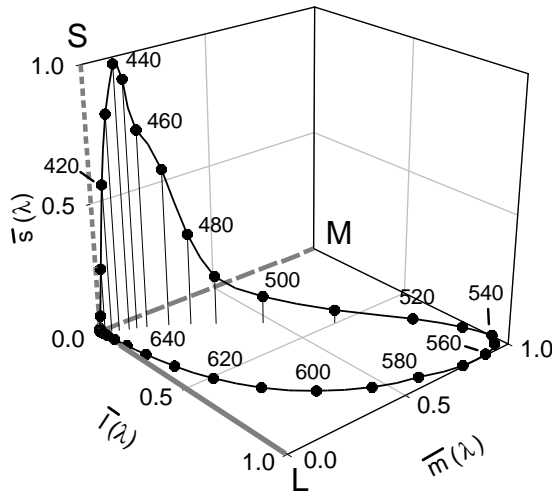


Figure 2.16: Cone fundamentals. Spectrum locus (continuous line) and selected wavelengths (filled circles) plotted in the Stockman and Sharpe (2000a) 2-deg $\bar{l}(\lambda)$, $\bar{m}(\lambda)$, and $\bar{s}(\lambda)$ cone excitation space, and the L- (solid gray line), M- (long-dashed gray line), and S- (short-dashed gray line) cone vectors.

the cone fundamentals and represent cone stimulation. Figure 2.16 shows the spectrum locus plotted in a three-dimensional 2-deg $\bar{l}(\lambda)$, $\bar{m}(\lambda)$, and $\bar{s}(\lambda)$ cone space.

The cone contrast space is a version of the cone fundamental space, in which the cone excitations produced by a stimulus are scaled separately for each cone type, according to Weber's law ($\Delta S/S$, $\Delta M/M$, and $\Delta L/L$, where ΔS , ΔM , and ΔL are the differential cone excitations produced by the stimulus, and S , M , and L are the unchanging cone excitations produced by, for example, a background). This space is useful for understanding postreceptoral mechanisms; it is discussed further in Chapter 18.

Equal-luminance cone excitation space. An oft referred to projection of the LMS cone space is the MacLeod–Boynton equal-luminance plane (Luther, 1927; MacLeod & Boynton, 1979), which is shown in Fig. 18.1B (see Chapter 18). Its popularity rests, in part, on current models about postreceptoral organization and, in particular, on the theory that only L- and

M-cones contribute additively to the luminance channel [see above, Luminosity channel, $V(\lambda)$].

The MacLeod–Boynton chromaticity coordinates are defined as:

$$(14) \quad r_{MB}(\lambda) = \frac{\bar{l}(\lambda)}{V(\lambda)},$$

$$g_{MB}(\lambda) = \frac{\bar{m}(\lambda)}{V(\lambda)}, \text{ and}$$

$$b_{MB}(\lambda) = \frac{\bar{s}(\lambda)}{V(\lambda)},$$

where

$$V(\lambda) = \bar{l}(\lambda) + \bar{m}(\lambda).$$

The MacLeod–Boynton coordinates can be calculated from the cone fundamentals and $V^*(\lambda)$, which are tabulated in the Appendix, or they can be obtained from our Web sites (see Appendix).

Other variations of this space have been proposed (Krauskopf, Williams, & Heeley, 1982; Derrington, Krauskopf, & Lennie, 1984). See also the Appendix by Brainard in Kaiser and Boynton (1996).

Concluding remarks

On the basis of extensive measurements in single-gene protanopes and deuteranopes, in blue-cone monochromats and in normals (Sharpe et al., 1998; Stockman & Sharpe, 2000a; Stockman, Sharpe, & Fach, 1999) we present the new L-, M-, and S-cone fundamentals shown in Fig. 2.12 and tabulated in the Appendix. We believe that these represent an improvement to the Smith and Pokorny (1975) fundamentals based on the Judd–Vos modified CIE 2-deg CMFs and a refinement of the Stockman, MacLeod, and Johnson (1993) fundamentals based on the CIE 10-deg CMFs corrected to 2 deg.

In the Appendix we present a consistent set of functions: the three cone fundamentals $\bar{l}(\lambda)$ (L-cone),

$\bar{m}(\lambda)$ (M-cone), and $\bar{s}(\lambda)$ (S-cone); the luminosity function, $V^*(\lambda)$; the lens density spectrum, $d_{lens}(\lambda)$; the macular density spectrum, $d_{mac}(\lambda)$; and the three photopigment optical densities, $\bar{l}_{OD}(\lambda)$, $\bar{m}_{OD}(\lambda)$, and $\bar{s}_{OD}(\lambda)$. These together can be used to define normal human color vision.

Acknowledgments

This work was supported by the National Institutes of Health grant EY 10206 awarded to AS, and by the Deutsche Forschungsgemeinschaft (Bonn) under grants SFB 340 Tp A6 and Sh23/5-1 and a Hermann-und Lilly-Schilling-Professor awarded to LTS. We thank Timothy Kraft for providing the suction electrode data, and Rhea Eskew, Jan Kremers, Anne Kurtenbach, Donald MacLeod, and Dan Plummer for comments. Rhea Eskew contributed substantially to the section on luminance. We also thank Sabine Apitz for help and encouragement.

Appendix

Table 2.1 (see next page) contains the proposed 2-deg cone spectral sensitivities: $\log L(\lambda)$ or $\log \bar{l}(\lambda)$, $\log M(\lambda)$ or $\log \bar{m}(\lambda)$, and $\log S(\lambda)$ or $\log \bar{s}(\lambda)$; luminosity function: $\log V^*(\lambda)$; photopigment optical densities: $\log \bar{l}_{OD}(\lambda)$, $\log \bar{m}_{OD}(\lambda)$, and $\log \bar{s}_{OD}(\lambda)$; and standard lens and macular densities. All cone spectral sensitivities and the luminosity function are in quantal units and are scaled to (interpolated) unity peak. To convert to energy units, add $\log(\lambda)$ and renormalize. The lens and macular densities are indepen-

dent of the units used.

The cone fundamentals were calculated using the Stiles and Burch (1959) 10-deg CMFs with $\bar{s}_G/\bar{s}_B = 0.010600$ for S, $\bar{m}_R/\bar{m}_B = 0.168926$ and $\bar{m}_G/\bar{m}_B = 8.265895$ for M, and $\bar{l}_R/\bar{l}_B = 2.846201$ and $\bar{l}_G/\bar{l}_B = 11.092490$ for L. For further details about the long-wavelength S-cone extension after 520 nm, see Stockman, Sharpe, and Fach (1999), who were unable to measure S-cone spectral sensitivity data after 615 nm [after which $S(\lambda)$ is so small that it can reasonably, for most purposes, be set to zero]. The photopigment optical density spectra were calculated using Eqns. (9) and (10) assuming peak photopigment optical densities of 0.40 for S, and 0.50 for L, M, and the tabulated macular and lens densities.

The Stiles and Burch 10-deg CMFs used to calculate the cone fundamentals are from Table I (5.5.4) of Wyszecki and Stiles (1982a), in which they are tabulated in wavelength steps of 5 nm, and from Tables 7 and 8 of Stiles and Burch (1959), in which they are tabulated in wavenumber steps of 250 or 500 cm^{-1} . At shorter wavelengths, we used the CMFs from Table I (5.5.4) (Wyszecki & Stiles, 1982a). Those CMFs, however, are uncorrected for rod intrusion and are tabulated only to four decimal places, which is too imprecise to define cone sensitivities at longer wavelengths. At longer wavelengths, therefore, we have corrected the original CMFs (Table 7 of Stiles & Burch, 1959) for rod intrusion (according to Table 8; Stiles & Burch, 1959) and reinterpolated them at 5-nm intervals. For further details, see Stockman and Sharpe (2000a).

The data contained in Table 2.1, and other information, are available on <http://www-cvrl.ucsd.edu> (USA) and on <http://www.eye.medizin.uni-tuebingen.de/cvrl> (Germany).

nm (λ)	$\log L(\lambda)$	$\log M(\lambda)$	$\log S(\lambda)$	$\log V^*(\lambda)$	$\log \bar{l}_{OD}(\lambda)$	$\log \bar{m}_{OD}(\lambda)$	$\log \bar{s}_{OD}(\lambda)$	lens $d_{lens}(\lambda)$	macular $d_{mac}(\lambda)$
	$\log \bar{l}(\lambda)$	$\log \bar{m}(\lambda)$	$\log \bar{s}(\lambda)$						
390	-3.2186	-3.2907	-1.9642	-3.2335	-0.9338	-1.0479	-0.1336	2.5122	0.0453
395	-2.8202	-2.8809	-1.5726	-2.8309	-0.8948	-0.9974	-0.0906	2.1306	0.0649
400	-2.4660	-2.5120	-1.2020	-2.4712	-0.8835	-0.9707	-0.0498	1.7649	0.0868
405	-2.1688	-2.2013	-0.8726	-2.1690	-0.9016	-0.9742	-0.0257	1.4257	0.1120
410	-1.9178	-1.9345	-0.5986	-1.9119	-0.9154	-0.9711	-0.0092	1.1374	0.1365
415	-1.7371	-1.7218	-0.3899	-1.7183	-0.9408	-0.9623	-0.0023	0.9063	0.1631
420	-1.6029	-1.5534	-0.2411	-1.5699	-0.9549	-0.9398	0.0000	0.7240	0.1981
425	-1.5136	-1.4234	-0.1526	-1.4627	-0.9576	-0.8990	-0.0054	0.5957	0.2345
430	-1.4290	-1.3033	-0.0821	-1.3617	-0.9536	-0.8564	-0.0222	0.4876	0.2618
435	-1.3513	-1.1899	-0.0356	-1.2668	-0.9390	-0.8027	-0.0499	0.4081	0.2772
440	-1.2842	-1.0980	-0.0004	-1.1874	-0.9267	-0.7627	-0.0810	0.3413	0.2884
445	-1.2414	-1.0342	-0.0051	-1.1338	-0.9041	-0.7159	-0.1199	0.3000	0.3080
450	-1.2010	-0.9794	-0.0260	-1.0859	-0.8734	-0.6675	-0.1665	0.2629	0.3332
455	-1.1606	-0.9319	-0.0763	-1.0417	-0.8335	-0.6174	-0.2395	0.2438	0.3486
460	-1.0974	-0.8632	-0.1199	-0.9756	-0.7801	-0.5543	-0.3143	0.2279	0.3500
465	-1.0062	-0.7734	-0.1521	-0.8852	-0.7211	-0.4924	-0.4008	0.2131	0.3269
470	-0.9200	-0.6928	-0.2145	-0.8019	-0.6643	-0.4374	-0.5165	0.2046	0.2996
475	-0.8475	-0.6300	-0.3165	-0.7346	-0.6122	-0.3925	-0.6623	0.1929	0.2842
480	-0.7803	-0.5747	-0.4426	-0.6736	-0.5515	-0.3405	-0.8161	0.1834	0.2786
485	-0.7166	-0.5234	-0.5756	-0.6163	-0.4871	-0.2850	-0.9679	0.1749	0.2772
490	-0.6535	-0.4738	-0.7169	-0.5600	-0.4289	-0.2378	-1.1316	0.1675	0.2688
495	-0.5730	-0.4078	-0.8418	-0.4867	-0.3618	-0.1821	-1.2887	0.1601	0.2485
500	-0.4837	-0.3337	-0.9623	-0.4048	-0.3040	-0.1384	-1.4581	0.1537	0.2093
505	-0.3929	-0.2569	-1.1071	-0.3208	-0.2499	-0.0980	-1.6570	0.1463	0.1652
510	-0.3061	-0.1843	-1.2762	-0.2406	-0.2007	-0.0644	-1.8804	0.1378	0.1211
515	-0.2279	-0.1209	-1.4330	-0.1693	-0.1558	-0.0383	-2.0865	0.1293	0.0812
520	-0.1633	-0.0699	-1.6033	-0.1109	-0.1093	-0.0095	-2.2925	0.1230	0.0525
525	-0.1178	-0.0389	-1.7853	-0.0719	-0.0771	0.0000	-2.5009	0.1166	0.0329
530	-0.0830	-0.0191	-1.9766	-0.0438	-0.0550	-0.0037	-2.7142	0.1102	0.0175
535	-0.0571	-0.0080	-2.1729	-0.0243	-0.0332	-0.0082	-2.9241	0.1049	0.0093
540	-0.0330	-0.0004	-2.3785	-0.0071	-0.0095	-0.0146	-3.1409	0.0986	0.0046
545	-0.0187	-0.0035	-2.5882	0.0000	0.0000	-0.0370	-3.3599	0.0922	0.0017
550	-0.0128	-0.0163	-2.8010	-0.0016	-0.0040	-0.0731	-3.5809	0.0859	0.0000
555	-0.0050	-0.0295	-3.0168	-0.0021	-0.0014	-0.1055	-3.8030	0.0795	0.0000

Table 2.1: Proposed 2-deg cone spectral sensitivities (continued on next page).

nm (λ)	$\log L(\lambda)$	$\log M(\lambda)$	$\log S(\lambda)$	$\log V^*(\lambda)$	$\log \bar{l}_{OD}(\lambda)$	$\log \bar{m}_{OD}(\lambda)$	$\log \bar{s}_{OD}(\lambda)$	lens $d_{lens}(\lambda)$	macular $d_{mac}(\lambda)$
	$\log \bar{l}(\lambda)$	$\log \bar{m}(\lambda)$	$\log \bar{s}(\lambda)$						
560	-0.0019	-0.0514	-3.2316	-0.0085	-0.0055	-0.1485	-4.0231	0.0742	0.0000
565	-0.0001	-0.0769	-3.4458	-0.0166	-0.0138	-0.1966	-4.2437	0.0678	0.0000
570	-0.0015	-0.1114	-3.6586	-0.0296	-0.0280	-0.2554	-4.4629	0.0615	0.0000
575	-0.0086	-0.1562	-3.8692	-0.0492	-0.0519	-0.3251	-4.6798	0.0551	0.0000
580	-0.0225	-0.2143	-4.0769	-0.0769	-0.0863	-0.4084	-4.8939	0.0488	0.0000
585	-0.0325	-0.2752	-4.2810	-0.1015	-0.1113	-0.4903	-5.1033	0.0435	0.0000
590	-0.0491	-0.3443	-4.4811	-0.1320	-0.1460	-0.5788	-5.3087	0.0381	0.0000
595	-0.0727	-0.4263	-4.6766	-0.1696	-0.1898	-0.6791	-5.5095	0.0329	0.0000
600	-0.1026	-0.5198	-4.8673	-0.2132	-0.2378	-0.7868	-5.7034	0.0297	0.0000
605	-0.1380	-0.6247	-5.0529	-0.2619	-0.2929	-0.9054	-5.8932	0.0254	0.0000
610	-0.1823	-0.7389	-5.2331	-0.3179	-0.3561	-1.0305	-6.0765	0.0223	0.0000
615	-0.2346	-0.8610	-5.4077	-0.3804	-0.4268	-1.1617	-6.2544	0.0191	0.0000
620	-0.2943	-0.9915		-0.4490	-0.5026	-1.2989		0.0170	0.0000
625	-0.3603	-1.1294		-0.5229	-0.5833	-1.4425		0.0148	0.0000
630	-0.4421	-1.2721		-0.6106	-0.6809	-1.5909		0.0117	0.0000
635	-0.5327	-1.4205		-0.7060	-0.7854	-1.7444		0.0085	0.0000
640	-0.6273	-1.5748		-0.8051	-0.8918	-1.9033		0.0053	0.0000
645	-0.7262	-1.7365		-0.9081	-0.9986	-2.0670		0.0042	0.0000
650	-0.8408	-1.8924		-1.0252	-1.1204	-2.2246		0.0032	0.0000
655	-0.9658	-2.0524		-1.1520	-1.2523	-2.3872		0.0011	0.0000
660	-1.0965	-2.2196		-1.2845	-1.3878	-2.5558		0.0000	0.0000
665	-1.2323	-2.3853		-1.4217	-1.5264	-2.7217		0.0000	0.0000
670	-1.3734	-2.5477		-1.5638	-1.6696	-2.8842		0.0000	0.0000
675	-1.5201	-2.7075		-1.7110	-1.8178	-3.0442		0.0000	0.0000
680	-1.6729	-2.8700		-1.8642	-1.9717	-3.2067		0.0000	0.0000
685	-1.8320	-3.0362		-2.0236	-2.1317	-3.3730		0.0000	0.0000
690	-1.9985	-3.2109		-2.1904	-2.2988	-3.5477		0.0000	0.0000
695	-2.1590	-3.3745		-2.3510	-2.4596	-3.7113		0.0000	0.0000
700	-2.3194	-3.5360		-2.5115	-2.6203	-3.8728		0.0000	0.0000
705	-2.4813	-3.6978		-2.6734	-2.7824	-4.0347		0.0000	0.0000
710	-2.6486	-3.8678		-2.8408	-2.9498	-4.2047		0.0000	0.0000
715	-2.8164	-4.0373		-3.0086	-3.1177	-4.3742		0.0000	0.0000
720	-2.9801	-4.1986		-3.1723	-3.2815	-4.5355		0.0000	0.0000
725	-3.1433	-4.3582		-3.3353	-3.4447	-4.6951		0.0000	0.0000
730	-3.3032	-4.5112		-3.4950	-3.6047	-4.8481		0.0000	0.0000

Table 2.1 (continued).

